Robotics and Autonomous Systems 202 (2026) 105486

Contents lists available at ScienceDirect

Robotics and Autonomous Systems

journal homepage: www.elsevier.com/locate/robot

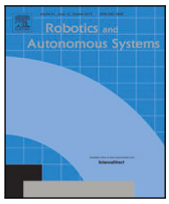

AITL-WING-HITL: Telemanipulation of autonomous drones using Digital Twins of aerial traffic interfaced With WING

Kaya Kuru [a,b,*], Sam Worthington [c], Darren Ansell [a], John M. Pinder [a], Aadithya Sujit [a], Benjamin J. Watkinson [a], Keith Vinning [d], Lee Moore [d], Chris Gilbert [d], David Jones [a], Claire Tinker-Mill [a]

[a] School of Engineering and Computing, University of Central Lancashire, Preston, PR1 2HE, UK
[b] Software Engineering Department, Fenerbahce University, Ataşehir, İstanbul, 34758, Turkey
[c] Worthington Sharpe Ltd., Unit 1.3s Halton Mill, Mill Ln, Halton, Lancaster LA26ND, UK [1]
[d] PilotAware Ltd., 19 John McGuire Crescent, Coventry, CV32Q, UK [2]

ARTICLE INFO

Keywords:
Teleoperation
Autonomous UAVs
Human-On-The-Loop (HOTL)
Human-In-The-Loop (HITL)
Autonomy-In-The-Loop (AITL)
Telerobotics
Digital Twins (DTs)

ABSTRACT

"By touching an instrument placed in the southern gallery, a miniature Spanish cruiser anchored in the fountain lake on the lower floor, 90 ft away, was blown into the air. There was no connection between the transmitter and the vessel in the lake," reported The New York Times in 1898. Though perceived as magic by many at the time, Nikola Tesla had once again pushed the boundaries of technology, becoming the forefather of modern remotely controlled wireless drones. His invention – an early radio-controlled vessel operated via radio waves – was hailed as "the first of a race of robots, mechanical men which will do the laborious work of the human race," and marked a leap far ahead of its time. Since then, human–robot interaction and the telemanipulation of drones have advanced substantially, especially in tandem with the evolution of autonomy. In this context, a scalable, agent-based platform – termed AITL-WING-HITL – was developed for the telemanipulation of Autonomous Unmanned Aerial Vehicles (A-UAVs) from the perspective of a human–multi-robot architecture, leveraging Digital Twins (DTs) of integrated aerial traffic. This system is designed to intervene in scenarios, where an autonomous AI agent – the "new driver" – encounters conditions too complex or unorthodox for autonomy alone to handle. The platform incorporates a patented, force-sensitive, precision control device known as the WING – an immersive tool tested with participants using measurable parameters to validate the system's effectiveness and identify areas for further improvement. The findings indicate that AITL (Autonomy-In-The-Loop) A-UAV agents and HITL (Human-In-The-Loop) Human Telemanipulator (HTM) agents can co-operate to achieve high-performance, synergistic task execution through a socio-cognitive interaction model embedded in the platform. By addressing current challenges and outlining directions for future exploration, this research not only provides an overview of the evolving landscape of drone telemanipulation but also serves as a roadmap for ongoing and future efforts in this critical field.

1. Introduction

"By touching an instrument placed in the southern gallery, a miniature Spanish cruiser anchored in the fountain lake on the lower floor, 90 ft away, was blown into the air. There was no connection between the transmitter and the vessel in the lake", reported The New York Times in 1898 [1]. Although many perceived it as magic, Nikola Tesla, once again pushing the boundaries of innovation, became the progenitor of modern-day remotely controlled wireless drones by inventing the first radio-controlled vessel using radio waves — an invention well ahead of its time [2]. This small radio-transmitting control box enabled Tesla to adjust the vessel's speed and direction by manipulating on-board mechanisms [3]. When a New York Times reporter described the

* Corresponding author at: School of Engineering and Computing, University of Central Lancashire, Preston, PR1 2HE, UK.
E-mail addresses: kkuru@lancashire.ac.uk, kaya.kuru@fbu.edu.tr (K. Kuru), sam@worthingtonsharpe.com (S. Worthington), dansell@lancashure.ac.uk (D. Ansell), jmpinder@lancashire.ac.uk (J.M. Pinder), asujit@lancashire.ac.uk (A. Sujit), bjwatkinson1@lancashire.ac.uk (B.J. Watkinson), keith.vinning@pilotaware.com (K. Vinning), lee.moore@pilotaware.com (L. Moore), chris.gilbert@pilotaware.com (C. Gilbert), djones38@uclan.ac.uk (D. Jones), cltinker-mill@lancashire.ac.uk (C. Tinker-Mill).

[1] https://www.worthingtonsharpe.com.
[2] https://www.pilotaware.com.

https://doi.org/10.1016/j.robot.2026.105486
Received 6 March 2024; Received in revised form 6 July 2025; Accepted 18 April 2026
Available online 24 April 2026

invention as a device "that could carry dynamite as a weapon of war", Tesla responded: "You do not see there a wireless torpedo; you see there the first of a race of robots, mechanical men – a borrowed mind (the machine's own mind) – which will do the laborious work of the human race" [4]. His vision foreshadowed today's multi-agent autonomous robotic systems, capable of remote operation via distinct frequencies. Tesla's U.S. patent (US613809 A) referred to the invention as a "distant operator" – what we now call a teleoperator [3]. Since then, remote human–robot interaction and telemanipulation have evolved significantly alongside advances in autonomy. Many large-scale and complex tasks now require remote operation supplemented by extended human intelligence and experience. Drones are increasingly deployed by organisations and companies to execute various missions – such as logistics deliveries [5] – and operate in autonomous modes Beyond Visual Line of Sight (BVLOS) along preplanned routes. These missions must be conducted safely, avoiding collisions with other aerial vehicles within integrated Unmanned Aerial Vehicle (UAV) Traffic Management (UTM) and Air Traffic Management (ATM) systems, collectively referred to as the UTM+ATM framework.

In all future visions involving networks of fully autonomous self-driving ground [6] or aerial vehicles [7], some form of remote human intervention is anticipated. Specifically, roles such as "Human-on-the-Loop" (HOTL) and "Human-in-the-Loop" (HITL) for telemonitoring and telemanipulation are expected to foster a desirable level of trust in autonomous vehicles (AVs) as they operate within highly dynamic urban or aerial environments [8]. Ensuring the safe and cost-efficient routing of Autonomous UAVs (A-UAVs) within the integrated UTM+ATM system requires strategic human oversight: HOTL for fully autonomous UAVs (FA-UAVs) and HITL for semi-autonomous UAVs (SA-UAVs), enabling humans to monitor and intervene when necessary (Fig. 15) – particularly when the Artificial Intelligence (AI) agent, acting as the new "driver", encounters unorthodox scenarios beyond the scope of its autonomy. As automation continues to evolve, the nature of human–machine interaction has fundamentally shifted beyond the traditional Humans-Are-Better-At/Machines-Are-Better-At (HABA/MABA) paradigm, in which humans and machines are often seen as competitors [9]. Instead, the Human-Agent-Robot Teamwork (HART) framework emphasises collaborative augmentation, where humans and machines co-work by leveraging their complementary strengths to enable practical and profitable applications [10]. This paper examines co-work within this HART-centric framework from the perspective of two intelligent, self-reliant entities: humans equipped with extended intelligence and experience, and A-UAVs operating with a high degree of autonomy. These two entities are critically interdependent for the successful management of rare and complex challenges. Throughout the paper, the "human teleoperator" (i.e. master) and the "in-vehicle teleoperator" (i.e. slave) are referred to as the "Human Telemanipulator" (HTM), acting as the HITL agent, and the "A-UAV" (FA-UAVs and SA-UAVs, i.e. AITL agents), respectively.

Manipulating A-UAVs BVLOS will remain a central topic in the coming years, particularly as autonomous systems increasingly take on indispensable roles in real-world applications. In alignment with this trajectory, the University of Lancashire is actively developing bespoke A-UAVs and AITL systems [3] through various funded projects,[4] aiming to tackle a wide range of complex operational tasks using A-UAVs. To support this mission, the University has partnered with PilotAware Ltd. and Worthington Sharpe Ltd. to ensure safe aerial operations, mitigating collision risks while enabling the execution of advanced aerial tasks. The core research question of this study is framed as follows: Can A-UAVs be effectively and efficiently manipulated through the collaborative operation of AITL and HITL agents? To explore this question, the following components were developed and integrated: (i) A Collision Management (CM) system, termed DACM (Drone Aware Collision Management) (Section 3.1.4), which creates Digital Twins (DTs) of aerial traffic through real-time communication with the decentralised PilotAware ATOM-GRID Network (Section 3.1.3); (ii) A patented, advanced force-sensitive control device, referred to as the WING, with 6DoF (Degree of Freedom) (Section 3.1.1), designed as an immersive precision-control interface for remotely operated vehicles (ROVs); (iii) A scalable agent-based platform – AITL-WING-HITL – that integrates these subsystems (Fig. 2) into a cohesive architecture, enabling HTMs to monitor and co-manipulate multiple A-UAVs within non-segregated aerial traffic environments, allowing human omnipresence.

While numerous novel robotic applications are anticipated, a range of emerging challenges must also be addressed — chief among them is ensuring that human–robot interaction remains safe, reliable, and effective [11]. One key question arises: Can the WING device facilitate effective interaction between HTMs and A-UAVs to accomplish tasks safely within the AITL-WING-HITL platform, especially given the potential limitations in human attention and perception when managing multiple A-UAVs simultaneously? To the best of our knowledge, this study represents the first comprehensive investigation into the use of a 6DoF advanced control device for manipulating multiple A-UAVs by a single HTM through digital replicas of aerial traffic, employing human–robot dialogue across several intervention modes (see Section 3.2.1). In addressing this research gap, the primary contributions of this paper are as follows:

(i) This research analyses the simultaneous manipulation of heterogeneous A-UAVs – autonomous aerial robots – by immersing HTMs within a newly integrated multi-agent architecture, termed AITL-WING-HITL.

(ii) The study explores the cooperative interaction between two intelligent entities – HTMs (HITL agents) and AITL AI agents – in performing complex tasks safely, accurately, and efficiently via various intervention modes (Fig. 15). This integration effectively bridges "the remote extension of human intelligence and expertise" with "vehicle autonomy".

The structure of the paper is outlined in Fig. 1 (see Table 1 for the abbreviations used in this paper).

2. Related works

A multitude of state-of-the-art studies have been conducted on the human telemanipulation of robots since the first teleoperator was built in the mid-1940s by Geortz [12]. Telerobotics, particularly bilateral robotic teleoperation activities between humans and robots, have generally been analysed based on the master and slave concept in which the slave side is mapped as "teleoperator" and the master side is mapped as "human operator" [8]. The supervisory role of human control in the remote manipulation of robots was first examined by Ferrell [13] in 1967. Most of the studies in the literature pay particular attention to HITL interactions, usually based on the semi-autonomous mode for human and single-machine hybrid activities to accomplish assigned tasks together, where semi-autonomous robotic systems are mainly designed with reliance on delay-tolerant human assistance [14]. The possibility of having multiple robots controlled by one operator (user) seems to be an additional crucial requirement in collaboration/cooperation [15]. Analysis of human–multirobot or human–multiagent cooperation and collaboration was immensely analysed in the 1990s as in [16–19], in particular, from the perspective of HITL decentralised systems, where the human needs to monitor the system all the time. The research of Nakauchi et al. [16] was the first in this direction in 1992. Laengle et al. [17] in 1997 had envisioned that "On one hand, robots have difficulties coping with unpredictable variations and uncertainties in their environment, which are normally no problem for humans. On the other hand, humans cannot always accomplish a task alone because of their limited force, slow execution

[3] https://www.lancashire.ac.uk/business/archive/lidz.

[4] https://www.lancashire.ac.uk/news/flying-high-universitys-drone-plans-boosted-through-investment.

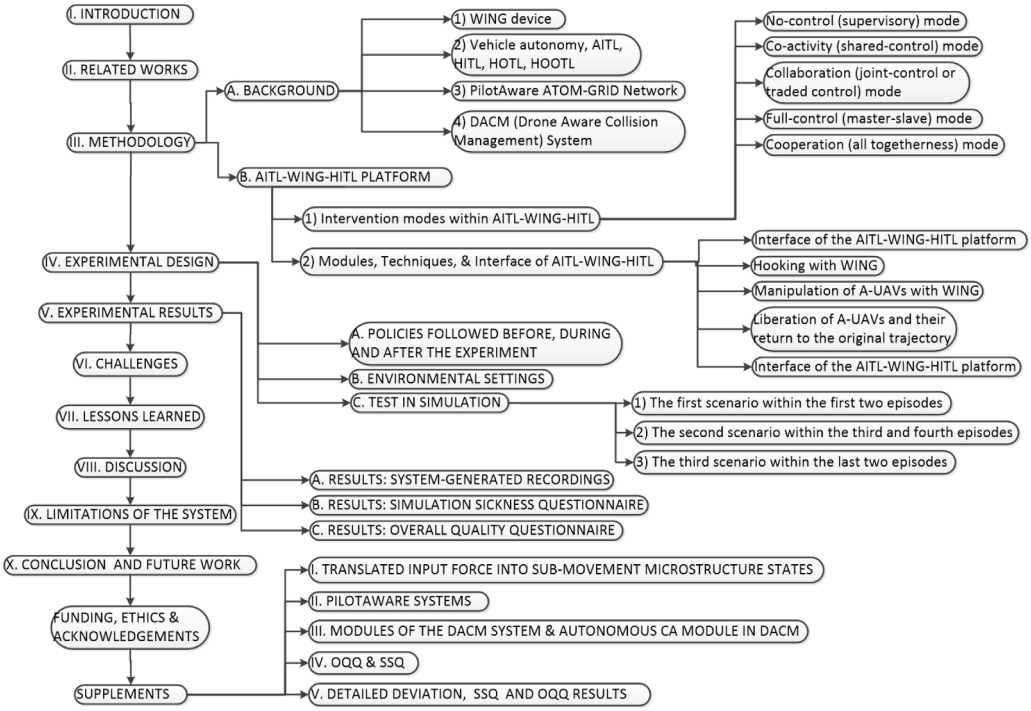

Fig. 1. Organisational structure of the paper.

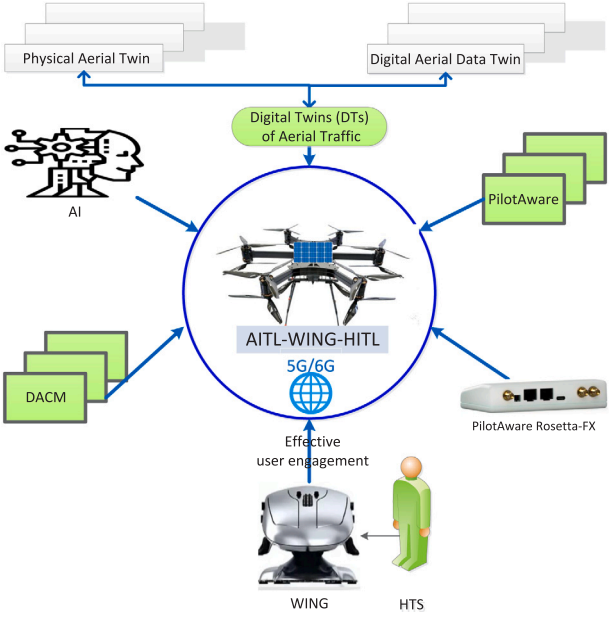

Fig. 2. Main building blocks of AITL-WING-HITL.

speed, limited working area, limited execution time, and low precision. By combining the complementary capabilities of the robot with those of the human within a team, new perspectives for mastering complex systems could be opened". The seeds of HOTL robot manipulation were placed by Suzuki et al. [17] in 1995 while analysing the cooperation between the human operator and the decentralised multi-agent robotic system. The research emphasises several principles of HOTL as "(1) the human operator usually does not control each agent in the system, (2) all information of the system is not concentrated in the human operator, (3) and the human operator needs not always watch over the system", "the human operator must know the status of the system when an urgent event occurs in the system and human intervention is required, or he is asked for some cooperation from agents". In a similar domain, this subject was extensively focused on during the 2000s while a mass number of robotic applications were taking their indispensable places. Fong et al. [20–23] closely scrutinised this subject and developed a framework in 2003 [21]. In the framework, how a few humans can teleoperate multiple teams of robots to accomplish the targeted task – that is, to assemble large orbital structures – was analysed. Later, human–robot teaming was focused on by Nourbakhsh et al. in 2005 [24] in real-world problem-solving applications, e.g. for urban search and rescue. The research on human–multirobot interaction in many disciplines has increased exponentially to solve real-world problems from the perspectives of HITL and HOTL since these preliminary works. Different types of immersive devices have been developed to interface with remote objects. Today's telemanipulation systems allow the interaction with environments at a distance and can also scale human force and motion to achieve stronger, bigger, or smaller action capabilities [25]. The study by Mithal et al. [26] suggests that joysticks are harder to control than mice. Martins et al. [27] concluded that participants' (with motor disabilities) feedback was more positive regarding 3D optical mice compared to the use of a conventional keyboard+mouse combination for navigation in 3D environments. The WING was tested in controlling 3D objects within computer-aided design (CAD) applications by Turner et al. [28], and by Sandoval et al. [29] in two short papers and found to be efficient in manipulating 3D virtual objects. Sandoval et al. [30], while testing several input devices with varying DoF, concluded that the more DoF available, the more enhanced the control over objects.

Human–drone interaction has been scrutinised by the research community to build easy-to-use interaction interfaces (e.g. natural interaction interfaces [31,32], touch-based [33]). The real-world telemanipulation initiatives with A-UAVs are expanding within the industry with the use of BVLOS, in particular, within the military industry. The aerial industry is partnering with leading telecommunication and technology companies that are experimenting with remote telemanipulation of A-UAVs in stochastic environments. Advanced multi-agent platforms, as well as hefty devices to interface with these platforms, are required

Table 1
Definitions of abbreviations.

No	Abbreviation	Definitions
1	ADS-B	Automatic Dependent Surveillance-Broadcast
2	AI	Artificial Intelligence
3	A-UAV	Autonomous Unmanned Aerial Vehicle
4	AoE	Automation of Everything
5	AITL	Autonomy-In-The-Loop
6	ATM	Air Traffic Management
7	AV	Autonomous Vehicle
8	BVLOS	Beyond Visual Line of Sight
9	CA	Collision Avoidance
10	CAD	Computer-Aided Design
11	CPS	Cyber-Physical System
12	CM	Collision Management
13	CVP	Cartesian Virtual Point
14	DACM	Drone Aware Collision Management
15	DRONEII	Drone Industry Insights
16	DoF	Degree of Freedom
17	DT	Digital Twin
18	EC	Electronic Conspicuity
19	ECG	ElectroCardioGram
20	EEG	Electroencephalogram
21	ERDF	European Regional Development Fund
22	EASA	European Union Aviation Safety Agency
23	FAUAV	Fully A-UAV
24	FL	Federated Learning
25	FoSR	Flight of Safety Route
26	GUI	Graphical User Interface
27	HART	Human-Agent-Robot Teamwork
28	HABA	Humans-Are-Better-At
29	HITL	Human-In-The-Loop
30	HOTL	Human-On-The-Loop
31	HTM	Human Telemanipulator
32	ICAO	International Civil Aviation Organisation
33	IcRz	Imminent-collision-Risk zone
34	IoE	Internet of Everything
35	ICTZones	Imminent Collision Travel Zones
36	MABA	Machines-Are-Better-At
37	MAV	Manned Aerial Vehicles
38	mm-WAVE	Millimetre-Wave
39	MEDL	Minimum Expected Deviation Level
40	mMTC	Massive Machine-Type Communications
41	PC-UAV	Pilot-Controlled UAV
42	PcRz	Probable-collision-Risk zone
43	PCTZone	Probable Collision Travel Cone
44	RoI	Region of Interest
45	ROV	Remotely Operated Vehicles
46	QoE	Quality of Experience
47	QoS	Quality of Services
48	QoT	Quality of Task
49	OGN	Open Glider Network
50	OQQ	Quality Assessment Questionnaire
51	SA-UAV	Semi A-UAVs
52	SSQ	Simulation Sickness Questionnaire
53	SA	Situation Awareness
54	SSA	State and Situation Awareness
55	SCS	Simulation and Cyber Sickness
56	SS	Simulation Sickness
57	STT	Safety Travel Tube
58	TL	Transfer Learning
59	TS	Total Score
60	UAV	Unmanned Aerial Vehicle
61	UTM	UAV Traffic Management
62	V2V	Vehicle-to-Vehicle
63	WLAN	Wireless Local Area Network

to extend human intelligence and experience for tele co-working with multiple A-UAVs to accomplish tasks as desired. In this sense, existing works on drone manipulation need to be extended to mitigate the aforementioned concerns. To this end, to the best of the observed knowledge, having received limited attention in the literature, telemanipulating A-UAVs through different intervention modes has not been analysed in-depth in the sense of establishing a holistic HITL/HOTL approach for improving co-work between humans and multiple A-UAVs, which makes this paper unique, aiming at closing this gap.

Fig. 3. WING device employed for Ground Based WING Station (GBS) using one hand.

3. Methodology

The integration of A-UAVs into non-segregated UTM+ATM aerospace environments necessitates unified platforms that support collective operations to ensure missions are carried out both efficiently and safely. Such platforms are essential for maintaining coordinated control of multi-DoF aerial vehicles while preserving safe separation distances. During the autonomous execution of multiple UAV missions – often orchestrated by different entities – unexpected events may arise, and individual missions cannot be treated in isolation, as they share the same aerospace infrastructure. This study aims to develop an integrated, collective framework that enables HITL and AITL agents to collaboratively manage uncertainty and execute autonomous missions effectively. The proposed approach supports global BVLOS operations by incorporating a comprehensive State and Situation Awareness (SSA) tracking system. The core components of the proposed platform – AITL-WING-HITL (Fig. 16) – for the manipulation of A-UAVs are illustrated in Fig. 2. At its foundation, the platform integrates the PilotAware system (Supplement II, Fig. 1) and the DACM system (Supplement III, Fig. 2) to generate DTs of aerial traffic. These primary components, along with supporting systems, are detailed in Section 3.1, prior to the full presentation of the developed platform in Section 3.2.

3.1. Background

Recent advances in Cyber-Physical Systems (CPSs) within the concepts of Internet of Everything (IoE) and Automation of Everything (AoE) [34] teleport us to teleoperate remote objects using DTs. In this treatise, the components of the designed platform which are depicted in Fig. 2 are explained in Sections 3.1.1, 3.1.2, 3.1.3, and 3.1.4 respectively and then the platform, as a holistic framework, is examined in 3.2.

3.1.1. WING device

The WING, a mouse-like, precision control device, was developed by Worthington Sharpe Ltd. in order to use the human motor system effectively. It is presented in Figs. 3, 4 with its functions. It, by extending the abilities of a mouse, combines the functions of a free-moving isotonic mouse and a free-flowing isometric joystick, leading to unprecedented freedom of movement from a desk-based control system. It enables movements in X, Y and Z directions as well as a complete precision roll (Φ), pitch (Θ) and yaw (Ψ) joystick functions as delineated in Fig. 5. The WING aims to create command and control solutions for ROVs and robotic equipment. The lower part contains the laser mouse sensor;

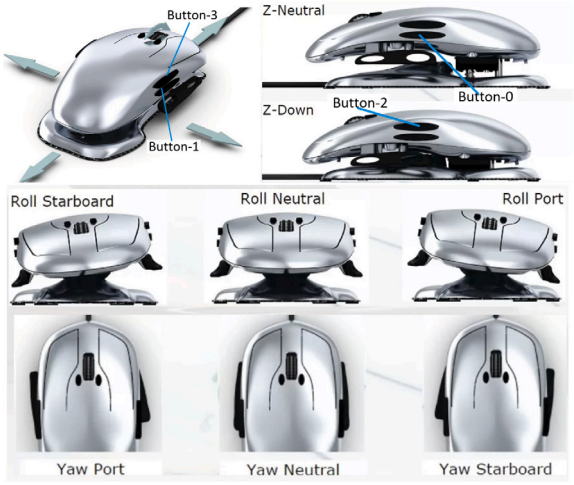

Fig. 4. Essential attributes: The mapping of the WING to the rotational orientations with three degrees — roll (Φ), pitch (Θ) and yaw (Ψ) channels.

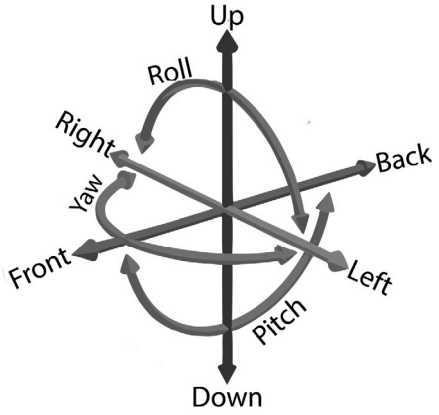

Fig. 5. Conceptualisation of 6DoF (i.e. 3 translation degrees and 3 rotation degrees) of the WING.

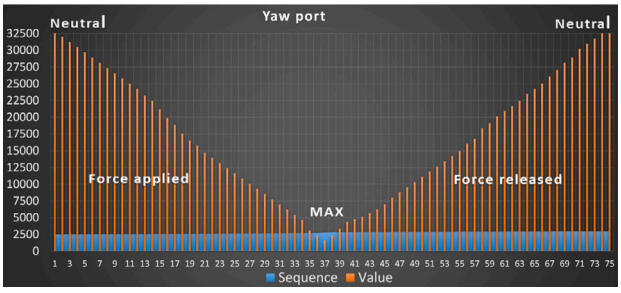

Fig. 6. States of Yaw Port (Table 2).

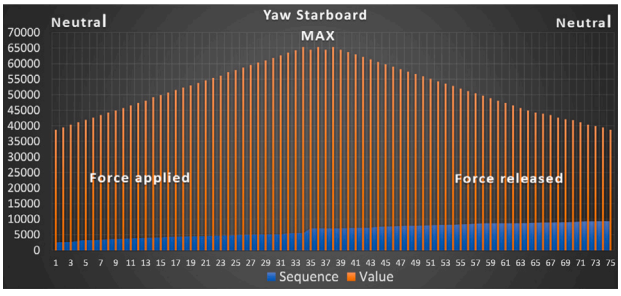

Fig. 7. States of Yaw Starboard (Table 2).

Table 2
Discrete microstructure movement (tele-impedance) of the WING in Yaw channel regarding the time and the subsequent sequences providing more information about the movement velocity over time: Port (Fig. 6); Blackboard (Fig. 7).

N	Yaw Port (RotationZ)			Yaw Starboard (RotationZ)			Force
	Seq	Timestamp	Value	Seq	Timestamp	Value	
1	2495	185 328 531	32 767	2416	266 585 875	38 749	Neutral
2	2496	185 328 537	31 993	2551	266 586 343	39 529	Applied
3	2499	185 328 546	31 219	2668	266 586 734	40 310	Applied
4	2502	185 328 546	30 445	2956	266 587 765	41 090	Applied
5	2503	185 328 562	29 671	3200	266 588 640	41 970	Applied
6	2508	185 328 578	28 897	3209	266 588 671	42 650	Applied
7	2515	185 328 593	28 123	3379	266 589 234	43 430	Applied
8	2520	185 328 609	27 349	3490	266 589 687	44 210	Applied
9	2526	185 328 625	26 575	3579	266 589 984	44 991	Applied
10	2533	185 328 656	25 801	3619	266 590 093	45 771	Applied
11	2537	185 328 671	25 027	3687	266 590 312	46 551	Applied
12	2542	185 328 687	24 253	3841	266 590 843	47 331	Applied
13	2545	185 328 703	23 221	3990	266 591 375	48 111	Applied
14	2548	185 328 718	22 447	4031	266 591 546	49 152	Applied
15	2555	185 328 734	21 141	4056	266 591 656	49 932	Applied
16	2557	185 328 750	19 867	4231	266 592 250	50 712	Applied
17	2559	185 328 750	18 835	4265	266 592 359	51 492	Applied
18	2562	185 328 781	17 545	4323	266 592 562	52 272	Applied
19	2565	185 328 796	16 513	4423	266 592 937	53 052	Applied
20	2566	185 328 796	15 738	4454	266 593 046	53 833	Applied
21	2577	185 328 828	14 706	4579	266 593 406	54 613	Applied
22	2582	185 328 843	13 932	4642	266 593 656	55 393	Applied
23	2589	185 328 875	13 158	4671	266 593 750	56 173	Applied
24	2601	185 328 906	12 384	4685	266 593 812	57 213	Applied
25	2606	185 328 921	11 610	4834	266 594 312	57 993	Applied
26	2610	185 328 937	10 836	4882	266 594 500	58 774	Applied
27	2618	185 328 953	10 062	4907	266 594 593	59 554	Applied
28	2621	185 328 968	9288	5069	266 595 125	60 334	Applied
29	2625	185 329 000	8514	5075	266 595 156	61 114	Applied
30	2632	185 329 015	7740	5086	266 595 187	61 894	Applied
31	2638	185 329 031	6966	5091	266 595 203	62 674	Applied
32	2647	185 329 062	6192	5416	266 596 406	63 455	Applied
33	2654	185 329 093	5418	5425	266 596 468	64 235	Applied
34	2662	185 329 125	4644	5428	266 596 468	65 275	Applied
35	2669	185 329 156	3096	7021	266 602 234	64 495	Applied
36	2676	185 329 187	2322	7024	266 602 250	65 275	Applied
37	2750	185 329 468	1548	7026	266 602 250	64 495	END
38	2828	185 329 687	2322	7031	266 602 281	65 275	Released
39	2832	185 329 703	3354	7047	266 602 343	64 495	Released
40	2833	185 329 718	4386	7094	266 602 531	63 715	Released
41	2836	185 329 726	4782	7188	266 602 890	62 934	Released
42	2839	185 329 734	5160	7197	266 602 906	62 154	Released
43	2841	185 329 742	5676	7203	266 602 937	61 374	Released
44	2843	185 329 750	6192	7526	266 604 062	60 594	Released
45	2847	185 329 765	6966	7638	266 604 453	59 814	Released
46	2856	185 329 781	7998	7694	266 604 671	59 034	Released
47	2860	185 329 796	8772	7795	266 605 015	58 253	Released
48	2864	185 329 812	9546	7837	266 605 140	57 473	Released
49	2868	185 329 812	10 320	7867	266 605 250	56 693	Released
50	2870	185 329 828	11 094	7904	266 605 390	55 913	Released

(*continued on next page*)

the upper part attaches via a precision slide and pivot mechanism to provide pitch, roll and z-height movement. Further control is then added through the under-slung yaw-bar positioned towards the front, giving a total of 6DoF. It, with advanced sensory mechanisms allowing precision control, was designed to address the needs of users who require the speed and accuracy of a high-end mouse for pointing and selection tasks, along with full 3D control. Additionally, it offers a wide range of buttons and a speed wheel that can be further programmed both to perform numerous functions and to map certain actions as we employ in this study. Readers are referred to the video[5] to observe how it functions with its particular features. Its particular functionalities

[5] https://www.worthingtonsharpe.com/wing.

Table 2 (*continued*).

51	2873	185 329 828	11 868	7976	266 605 703	55 133	Released
52	2881	185 329 859	12 642	8066	266 606 015	54 353	Released
53	2886	185 329 875	13 416	8135	266 606 250	53 572	Released
54	2890	185 329 890	14 190	8148	266 606 296	52 792	Released
55	2896	185 329 906	14 964	8337	266 606 953	52 012	Released
56	2900	185 329 921	15 996	8389	266 607 125	51 232	Released
57	2903	185 329 921	16 771	8517	266 607 593	50 452	Released
58	2907	185 329 937	18 319	8591	266 607 859	49 672	Released
59	2911	185 329 953	19 093	8617	266 607 953	48 891	Released
60	2912	185 329 953	20 125	8619	266 607 968	48 111	Released
61	2913	185 329 968	20 899	8623	266 607 984	47 331	Released
62	2914	185 329 968	21 673	8627	266 608 000	46 551	Released
63	2915	185 329 984	22 447	8638	266 608 031	45 771	Released
64	2920	185 330 000	23 479	8659	266 608 093	44 991	Released
65	2922	185 330 015	24 253	8890	266 608 890	44 210	Released
66	2925	185 330 015	25 027	8912	266 589 687	43 918	Released
67	2931	185 330 046	26 059	8948	266 609 093	43 430	Released
68	2932	185 330 046	27 091	8961	266 609 125	42 650	Released
69	2934	185 330 062	28 123	8997	266 609 317	42 112	Released
70	2935	185 330 062	28 897	9049	266 609 437	41 870	Released
71	2937	185 330 078	30 187	9183	266 609 906	41 090	Released
72	2939	185 330 078	30 961	9254	266 610 187	40 310	Released
73	2940	185 330 078	31 735	9271	266 610 221	39 910	Released
74	2941	185 330 093	32 767	9287	266 610 312	39 529	Released
75	2942	185 331 062	32 767	9296	266 610 343	38 749	Neutral

regarding the primary objectives of this research can be summarised as follows.

(i) Multiple A-UAVs can be hooked and manipulated separately by the same hand.

(ii) A-UAVs can be directed using pre-defined navigation waypoints, and their trajectories can be adjusted during the mission.

(iii) Integrated 4-axis joystick functionality allows for performing various actions synchronously, such as simultaneous mission planner operation, camera gimbal control, flight path adjustments, or full manual piloting.

(iv) Joystick functions can be integrated into APM Planner 2.0, Ardupilot Mission Planer, DJI Ground Station, and any independent Ground Control Station (GCS) that supports standard joystick inputs (Fig. 3).

(v) Familiar computer mouse shape, speed, and accuracy reduce the learning curve, allowing the operator to focus on the task promptly during telemanipulation.

The min and max values of the rotational orientations — roll (Φ), pitch (Θ) and yaw (Ψ) are shown in Table 3. The WING's motions with discrete microstructure values can be mapped into the manoeuvres of A-UAVs. The Yaw states of the WING detected by the developed application in this research are shown in Table 2, and their graphical representations are depicted in Fig. 6 for Yaw Port and Fig. 7 for Yaw Starboard. The acquired sequences and the time are incorporated to visualise how the velocity varies over the duration of the force applied and released. The readers are referred to Supplement I for all the translated input forces (Fig. 4) into sub-movement microstructure states.

3.1.2. Vehicle autonomy, AITL, HITL, HOTL, and HOOTL

The exponential growth of interest and research in UAVs is strongly pushing for the emergence of autonomous flying robots [35]. 10 control levels of UAV swarms from fully supervisor-controlled to fully autonomous mode between human and machine were analysed in [36]. Drone Industry Insights (DRONEII) categorises the autonomy with 5 levels [37] based on degrees of independence, namely, 1: low automation (i.e. the UAV has control of at least one vital function, with a pilot in control); 2: partial automation (i.e. the UAV can take over heading and altitude under certain conditions with a pilot still responsible for safe operation); 3: conditional automation (i.e. the UAV can perform all functions and a pilot acts as a fall-back system); 4: high automation (i.e. the UAV has back-up systems, so if one fails, the platform is still

Table 3
WING min and max values of the rotational orientations — roll (Φ), pitch (Θ) and yaw (Ψ).

Orientation	WING	WING State	Min/Max	Parameter	Value
Yaw (Ψ)	Yaw Port	RotationZ	Max	Ψ_{Pmax} =	32 767
Yaw (Ψ)	Yaw Port	RotationZ	Min	Ψ_{Pmin} =	1548
Yaw (Ψ)	Yaw Starboard	RotationZ	Max	Ψ_{Smax} =	64 495
Yaw (Ψ)	Yaw Starboard	RotationZ	Min	Ψ_{Smin} =	38 749
Roll (Φ)	Roll Port	X	Max	Φ_{Pmax} =	60 074
Roll (Φ)	Roll Port	X	Min	Φ_{Pmin} =	37 189
Roll (Φ)	Roll Starboard	X	Max	Φ_{Smax} =	36 149
Roll (Φ)	Roll Starboard	X	Min	Φ_{Smin} =	3870
Pitch (Θ)	Pitch Forward	Y	Max	Θ_{Fmax} =	37 709
Pitch (Θ)	Pitch Forward	Y	Min	Θ_{Fmin} =	10 836
Pitch (Θ)	Pitch Backward	Y	Max	Θ_{Bmax} =	62 414
Pitch (Θ)	Pitch Backward	Y	Min	Θ_{Bmin} =	39 790

operational while a pilot is out of the loop); 5: full automation (i.e. the UAV can plan its actions using advanced AI learning techniques) with little to no human intervention in the control loop. As the level of autonomy increases, UAVs can operate in more complex environments and execute more complex tasks with less prior knowledge and fewer operator interactions [38].

AI agents are now capable of intentionally constraining, complementing, or substituting human involvement in the execution of routine tasks [39]. With Human-out-of-the-Loop (HOOTL) systems, AI agents are expected to execute assigned tasks without human intervention. Humans and machines may need to work hand-in-hand to complete numerous tasks safely, accurately, efficiently, and ethically, in particular, for safety-critical jobs requiring a high level of precision. HITL interaction, requiring active human involvement, is employed for the systems by which a task may not be achieved either by a human or a machine. The concept of HITL dates back to the early 1940s, when humans primarily served as error detectors, monitoring systems and intervening when necessary [40]. HITL, i.e. hands-on, system allows humans to monitor the actions continuously, interact with the system and manipulate decisions that do not seem to be an optimal outcome or situations that involve nondeterministic behaviours of AI. SA-UAVs require humans (HITL) and onboard AI (AITL) to interact with each other continuously, where uncertainty is possible to emerge. In other words, there is always a person or people watching the HITL system actively, in which SA-UAVS are mainly involved, to intervene to fix any problem that is expected to occur. On the other hand, there is no need to employ a person to monitor FA–UAVS. However, it's still best to have a person as HOTL passively for remote monitoring to easily step in when alerted by the AI agent and manipulate when autonomy – AITL – encounters uncertainty about what to do next. HOTL interaction turns into HITL when the human agent is alerted. However, HITL is a phase that continues until an alerted uncertainty is handled, and the system turns into the HOTL interaction after the job has been completed. In 2025, the London Office of Technology and Innovation (LOTI) launched a research project to explore the role of HITL, prompted by ongoing questions about what constitutes meaningful human involvement and how effective the designated individual is in mitigating the ethical risks associated with AI [41]. Generally speaking, HOTL/HITL systems are utilised to ensure the expected automated behaviour of A-UAVs and consequently to ensure aerial traffic safety as well as ground-based safety. HOTL systems, while operating with little to no human intervention and not requiring to be alerted all the time, still allow HTMs to perform other tasks while the autonomy level of decentralised agents is relied on to accomplish assigned missions/tasks. HTMs monitor A-UAVs during the progress of the assigned missions within the HITL system. HITL, where a HTM is supposed to be on alert all the time to fix any emerging problem that the vehicle cannot cope with, is commonly used in controlling level-3 and level-4 autonomy. A level-5 autonomy can perform under all predefined circumstances and conditions. In this regard, this paper focuses on both HOTL and HITL with A-UAVs, where

Table 4
Data Streaming from the PilotAware system: Instant flight information. The value of the instant data capture in time, epoch (i.e. Unix timestamp), 162 522 6964, equals "Fri Jul 02 2021 12:56:04 GMT+0100 British Summer Time".

	Time (epoch)	Transponder	Receiver	Latitude	Longitude	Altitude (Feet)	Heading	Speed (knots/h)	Call sign
Example 1	162 522.964	401B8D	ADB	52.08688	0.170053	1100	237	88	GBCOU

Fig. 8. PilotAware small lightweight Rosetta-FX graffiti module, combining all EC technologies together and enabling seamless Flarm Integration, can detect all EC types including ADS-B, Sky Echo, PilotAware, Mode-S with Weather RADAR and Enhanced Traffic Data.

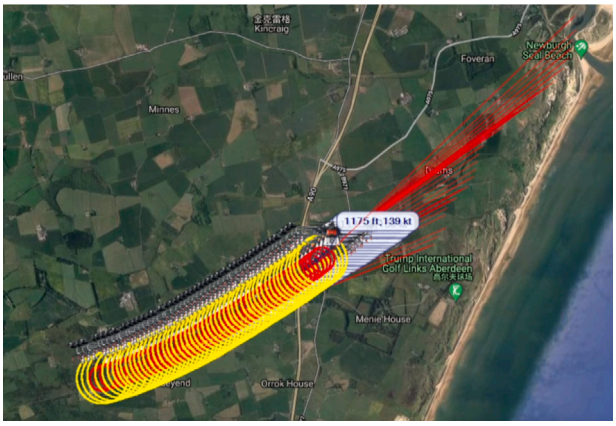

Fig. 9. Generation of future waypoints: safety travel tube with estimation-based predictive display.

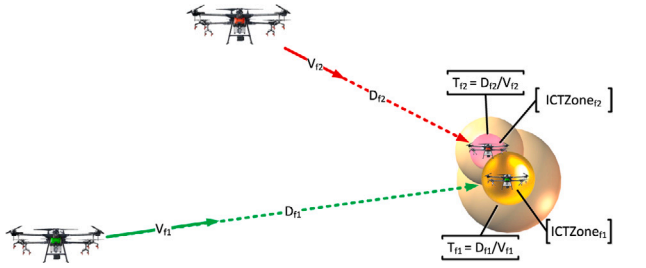

Fig. 10. Estimation-based predictive display: Early warning for a collision risk concerning an impending crossing point (impending crossing within $IcRz$) with two flights that have different velocities and are flying at similar altitudes. V, D and T correspond to "velocity", "distance" and "time to reach the crossing point" respectively.

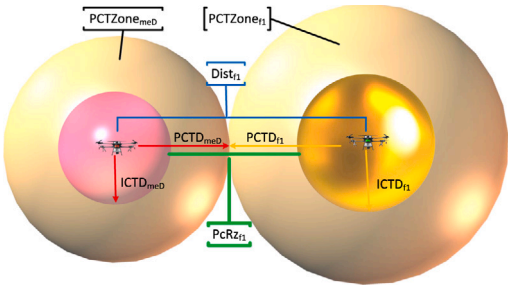

Fig. 11. Alert-YELLOW: Conflict geometry of $PCTD$ and $PcRz$: The yellow zone for each flight represents $PCTZone$. The red zone for meD and the orange zones for other flights represent $ICTZones$. (For interpretation of the references to colour in this figure legend, the reader is referred to the web version of this article.)

the HTM is expected to intervene remotely in rare difficulties that the vehicle cannot tackle under exceptional conditions. Autonomy has changed the relationship between humans and robots extensively. They are becoming more harmonious while taking part in specific task executions as the level of autonomy increases with further intelligence. This relationship is elaborated in Section 3.2.1 with various intervention modes. It must be noted that the HOTL/HITL manipulation through the intervention modes is performed if necessary, and AITL is expected to take over the HTM completely as soon as possible to realise the main objective of autonomy – self-reliance and self-governing (see Fig. 8 for the EC device and Table 4 for a data instance example acquired from the EC device).

3.1.3. PilotAware ATOM-GRID Network

The PilotAware ATOM-GRID Network (i.e. currently over 320 UK ATOM stations) is elaborated in Supplement II. The network detects aircraft that transmit any of the various Electronic Conspicuity (EC) signals used in Europe. These include ADS-B (Automatic Dependent Surveillance-Broadcast), CAP 1391 and Mode-S signals on the ICAO (International Civil Aviation Organisation) aviation band and Flarm, PilotAware, Fanet + and OGN (Open Glider Network) trackers that use the EASA (European Union Aviation Safety Agency) SRD 860 Band. Aircraft that transmit using the SafeSky mobile app are also detected.

3.1.4. DACM (Drone Aware Collision Management) system

The DACM system was developed to monitor aerial traffic and trigger autonomous cooperative manoeuvres that consider the aerodynamic, flight dynamics and particular features (e.g. physics, kinematics, manoeuvrability) of A-UAVs as mobile aerial agents within a multi-disciplinary joint project [42]. This system is illustrated in Supplement III (Fig. 2). The interface of this system, equipped with simulation capabilities and low-cost equipment, provides us with a full range of testing capabilities in both real-world applications of A-UAVs and co-simulation environments. The DACM – that is tightly coupled with the PilotAware ATOM-GRID Network (Section 3.1.3) – collects instant operational manoeuvre information from all aerial vehicles via simultaneous low-bandwidth data streams from each of the aerial vehicles. The low-bandwidth dual-path data communication is also mainly used in this research for conveying HTM command messages (e.g. new_heading = heading + 15) and necessary telemetry data (e.g. battery level of A-UAVs). The DACM – a digital replica of aerial traffic – integrates all near-real-time streamed data within its DT counterpart for convenient monitoring with more immersive telepresence for HTMs. Autonomous actuation for A-UAVs is performed to avoid emerging hazards in this immersive interface. The DACM supports HTMs to perceive the remote aerial traffic with effective SSA. The main features are outlined as follows.

1- The DACM, equipped with a novel CM methodology within an autonomy control framework using geometry formation of flights, enables BVLOS operations with collision-free trajectories.

2- The system, with (i) perception, (ii) decision-making, and (iii) automated actuation phases, can perceive the surrounding dynamic environment precisely using a global coverage strategy requiring no sophisticated sensors and react efficiently to multiple non-linear collision risks at a time with minimum trajectory deviations, requiring no prior training.

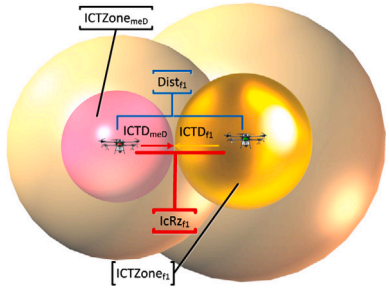

Fig. 12. High-alert-RED: Conflict geometry of $ICTD$ and $IcRz$.

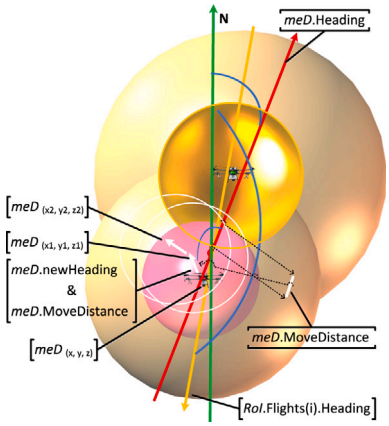

Fig. 13. Geometric illustration of CA manoeuvres (Supplement III, Alg. 2). $meD.MoveDistance$ is corresponding to the invasion length of the $ICTZones$.

3- The DACM in both air-only and air/ground modes not only implements Collision Avoidance (CA) for FA-UAVs, but also manages Pilot-Controlled UAVs (PC-UAVs) in improving operational safety, where it might be difficult for pilots to detect surrounding close-range/high-speed flights (see Fig. 13 for the geometric illustration of CA manoeuvres).

$$\begin{aligned} PcRz_{f1} ==> (Dist_{f1} \le PCTD_{meD} + PCTD_{f1}) \;\&\; \\ (Dist_{f1} > ICTD_{meD} + ICTD_{f1}); \\ where\,(0 < P_c \le 0.5) \;\&\; (PCTD = 2\ X\ ICTD) \end{aligned} \tag{1}$$

$$\begin{aligned} IcRz_{f1} ==> (Dist_{f1} \le ICTD_{meD} + ICTD_{f1}) \;\&\; (Dist_{f1} > 0); \\ where \quad (0.5 < P_c \le 1) \;\&\; (PCTD = 2\ X\ ICTD); \end{aligned} \tag{2}$$

$$\begin{aligned} ICTZone = \frac{4}{3}\pi(ICTD)^3; \\ PCTZone = (\frac{4}{3}\pi(PCTD)^3) - ICTZone = \frac{28}{3}\pi(ICTD)^3; \end{aligned} \tag{3}$$

$$\begin{aligned} \mathbf{CALatR} = \sin^{-1}(\sin(latR) * \cos(distCARadius) \\ + \cos(latR) * \sin(distCARadius) * \cos(bearingCAR)); \\ \mathbf{CALonR} = LonR + \tan^{-1}(\sin(bearingCAR) * \sin(distCARadius) \\ * \cos(latR))/(\cos(distCARadius) - \sin(latR) * \sin(meCALat)); \\ \underline{\mathbf{meDCALat}} = CALatR * (180/\pi); \underline{\mathbf{meDCALon}} = CALonR * (180/\pi); \\ \mathbf{where}\, latR = meLat * (\pi/180); lonR = meLon * (\pi/180); \\ bearingCAR = newHeading * (\pi/180); \\ distCARadius = MoveDistance/EarthRadius; \end{aligned} \tag{4}$$

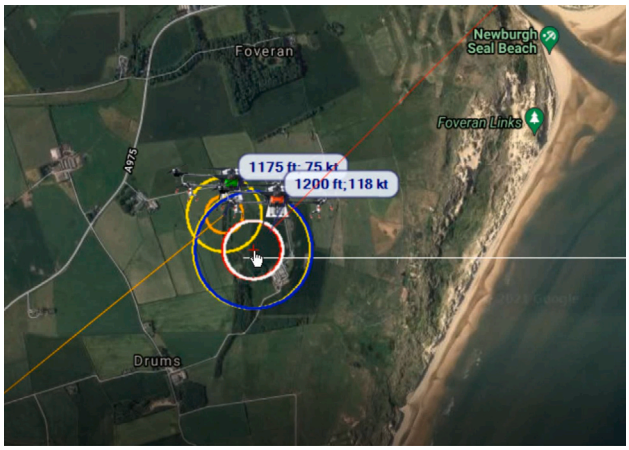

Fig. 14. Self manoeuvring using the simulated and real flight data: Red $ICTZone$ and heading and yellow $PCTZone$ within the original path; white $ICTZone$ and heading and blue $PCTZone$ within the manoeuvring trajectory. (For interpretation of the references to colour in this figure legend, the reader is referred to the web version of this article.)

The modules of the DACM, allowing autonomous navigation for A-UAVs with appropriate actuation mechanisms by coordinating the actions of multiple heterogeneous A-UAVs, are introduced in Supplement III, and the methodology using these modules is depicted in Supplement III (Fig. 2). In addition to autonomous actuation mechanisms to avoid any collision risk, the DACM system alerts the HOTL/HITL HTM if any flight is departing from its pre-planned trajectory, where the two control inputs (i.e. pre-planned waypoints and active waypoints) do not agree, considering that a probable failure is causing this unexpected manoeuvre under no collision risk using the health assessment and failure detection module.

The main goal of CM is to keep flights away from hazardous regions with conflict-free solutions at the very early stage by keeping each flight well clear of other traffic, considering their current trajectories and preplanned routes. Currently, A-UAVs do not have a system that will warn an operator of an impending collision with other airborne vehicles [43] using broader local coverage. In this module, SSA through horizontal and vertical planes is provided with the active flights and early collision risk assessment is processed, considering their trajectory predictions. From a linear formulation technical viewpoint, the flights' time-invariant connectivity of previous waypoints, their trajectory headings and their Probable Collision Travel Cone ($PCTZone$) and Imminent Collision Travel Zones ($ICTZones$) are used to generate the projections of future linear or non-linear waypoints (e.g. kinematic Cartesian Virtual Points (CVPs)), leading to a Safety Travel Tube (STT) using an estimation-based predictive display as depicted in Fig. 9. A-UAVs are said to be within Flight of Safety Route, i.e. $FoSR$, where there are no overlapping STTs as shown in Fig. 10 with estimation-based predictive directions. The DACM is responsible for instructing the flight controller, i.e. HTM, to maintain A-UAV separation from conflicting regions with a conflict resolution mechanism and to avoid imminent collisions autonomously. The HTM with HOTL mode is first informed about the approaching collision risk if STTs of flights are intersecting at a crossing point, considering the conflict geometry regarding the velocities, heading and altitudes. The system turns into the HITL state, where there is a crossing point indicating an impending collision risk. The system, second, warns for the probable collision risks (within Probable-collision-Risk zone ($PcRz$)) as illustrated in Fig. 11. Third, it alerts for imminent collision risks (within Imminent-collision-Risk zone ($IcRz$)) as illustrated in Fig. 12 along with autonomous deconflicting manoeuvres (Fig. 14).

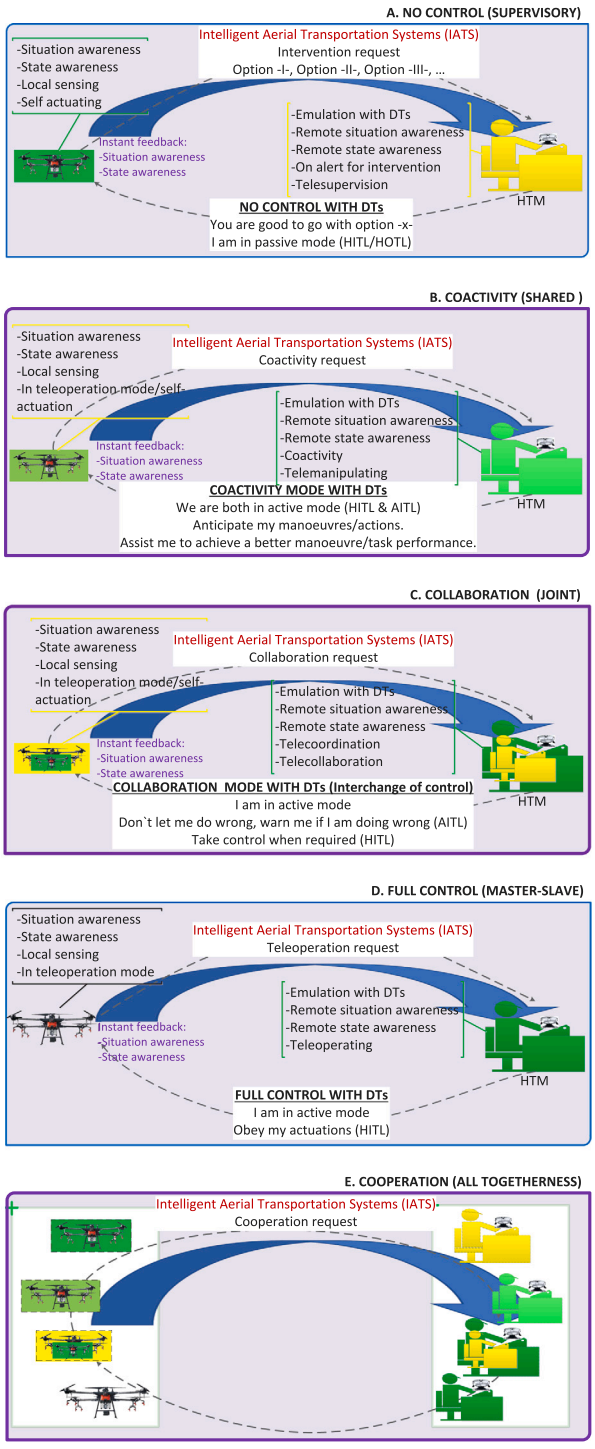

Fig. 15. HITL/HOTL interaction with a high level of transparency. Intervention modes: "No-control (supervisory)", "co-activity (shared)", "collaboration (joint)", "full control (master–slave)", and "cooperation (all togetherness)".

3.2. AITL-WING-HITL platform

Fatigue, lack of concentration, and poor displays all contribute to reduced performance in telemanipulating remote objects, and humans have difficulty building mental models of remote environments [20]. Therefore, these shortcomings must be compensated for with the establishment of easy-to-use interfaces, enabling robust interaction between AITL AI agents and remote human cognitive intelligence. Most importantly, two intelligent nodes – A-UAV and skilled HTM – have to be tightly coupled with human-oriented and vehicle-centric interfaces by exploiting the smartness at the vehicle end. The remote environment of A-UAVs should be observed by HTMs using constant dynamic SSA to generate proper commands at the appropriate time.

The AITL-WING-HITL platform aims to provide a tightly coupled interface between two intelligent agents — HOTL/HITL HTM and onboard aerial AITL AI agent from a multi-agent manipulation perspective. It encompasses a variety of human–robot co-work technologies that enable various interaction modes (elaborated in Section 3.2.1) and guarantee seamless transitions between these modes whenever they are needed. Technically speaking, the platform provides the HTM with a high degree of immersiveness ability with the established DTs of aerial traffic to enable the HTM to both perfectly perceive the remote aerial traffic with a full sense of telepresence (e.g. transparency) and track the results of their manipulated discrete microstructure actuation (i.e. teleimpedance) with back-feeding by incorporating a large set of integrated components as shown in Fig. 2. These integrated components mainly allow the user to interact with precision (e.g. correct aerial information with the PilotAware network (Supplement II, Fig. 1)), real-time user tracking of aerial traffic supported by a large set of proactive AI implementations (e.g. early warning, CA) with the DACM (Supplement III (Fig. 2)) and 6DoF in manipulation with the WING (Figs. 4, 5) as well as its discrete microstructure movement (Figs. 6, 7, Table 2). First, we would like to examine the co-work aspects of two intelligent entities theoretically through different intervention modes (Fig. 15) in Section 3.2.1 before delving into the merits of AITL-WING-HITL in Section 3.2.2.

3.2.1. Intervention modes within AITL-WING-HITL

A-UAVs operate autonomously and need to receive assistance whenever necessary. Time-varying delays are inevitable during the co-work interaction regarding the communication time delay problem, decision-making delays regarding the Quality of Experience (QoE) of HTMs and the evaluation of the voluminous sensor data and actuation time delays; Moreover, human remote intervention is vulnerable to human decision errors regarding incomplete environmental information based on the current state and imminent states of the vehicle concerning the other traffic participants, obstacles and hazards [8]. Even with a high level of SSA, human telemanipulation is strictly dependent on the cognitive and perceptual capabilities, spatial orientation abilities and motor skills of HTMs to avoid risky manoeuvres [8]. To this end, it is important to use the intelligence at the remote site, and it is advantageous to co-work during the execution of the complex tasks that cannot be handled by autonomy.

If A-UAVs are capable of performing on their own, human intervention is not needed, allowing HOTL systems, particularly with FA–UAVs. Otherwise, a remote extension of human intelligence and expertise with HITL interaction may be necessary either for better task performance to avoid disastrous situations during possibly hazardous operations or for executing very complex tasks beyond the capabilities of autonomy. The WING, with 6DoF, allows a HTM, with superior motor capabilities and perception/interpretation/implementation skills, to have partial or total control of A-UAVs to achieve their tasks safely and efficiently. With the help of the WING, HITL HTM inputs range with discrete microstructure values as depicted in Table 2, considering the intervention modes ranging from "no-control (supervisory) mode" to "full-control (master–slave) teleoperation mode" as delineated in Fig. 15. These intervention modes are elaborated in our previous study in [44]. These modes are summarised below in their dedicated subsections. The WING allows a HTM to switch between AITL and HITL states as well as between the interaction modes. The AITL-WING-HITL platform provides HTMs and AI agents with a high level of transparency through these interaction modes to work together with a high degree of efficacy. The WING, interfaced with AITL-WING-HITL, coordinates the tasks/subtasks by

Table 5
Main distinctive features of the intervention modes.

	Loop	Decision	Obedience A-UAV	Obedience HTM	Solution for conflicts	Full control	Built-in safety mechanism
No-control (supervisory)	HITL	HTM	Yes	No	N/A	Yes (A-UAV)	Operational
co-activity (shared-control)	HITL & AITL	HTM & A-UAV	No	Yes	HTM & A-UAV	No	Operational
Collaboration (joint-control)	HITL || AITL	HTM || A–UAV	No	No	HTM || A-UAVs	Partial	Operational
Full-control	HITL	HTM	Yes	No	N/A	Yes (HTM)	Inactive
Cooperation (all togetherness)	Mix interactions	Mix modes (above)	Mix modes (Yes || No)	Mix modes (Yes || No)	Mix modes (above)	Mix modes(above)	Operational

Table 6
Transition responsibilities for the intervention mode switching.

Switching decision	Current control	Next control	Current dominance	Next dominance	Switching control
No » » co-activity	A-UAV	A-UAV-HTM	A-UAV	A-UAV&HTM	A-UAV
No » » collaboration	A-UAV	A-UAV-HTM	A-UAV	HTM	A-UAV&HTM
No » » full	A-UAV	A-UAV-HTM	A-UAV	HTM	A-UAV&HTM
Co-activity » » collaboration	A-UAV-HTM	A-UAV-HTM	A-UAV&HTM	HTM	HTM
Co-activity » » full	A-UAV-HTM	A-UAV-HTM	A-UAV&HTM	HTM	HTM
Co-activity » » no	A-UAV-HTM	A-UAV	A-UAV&HTM	A-UAV	A-UAV
Collaboration » » full	A-UAV-HTM	A-UAV-HTM	HTM	HTM	HTM
Collaboration » » no	A-UAV-HTM	A-UAV	HTM	A-UAV	HTM&A-UAV
Collaboration » » co-activity	A-UAV-HTM	A-UAV-HTM	HTM	A-UAV&HTM	HTM
Full » » no	A-UAV-HTM	A-UAV	HTM	A-UAV	HTM&A-UAV
Full » » co-activity	A-UAV-HTM	A-UAV-HTM	HTM	A-UAV&HTM	HTM
Full » » collaboration	A-UAV-HTM	A-UAV-HTM	HTM	HTM	HTM

effectively modulating the HTM's hand tele-impedance in a smooth, goal-oriented manner based on the required behaviours of the intervention mode in action and the task to be accomplished. The HTM with the HOTL interaction mode can change the state to HITL to monitor the aerial traffic at any time and take action in one of the intervention modes to ascertain aerial safety or to accomplish any particular tasks. Then, the HITL state can be switched to the HOTL state after any uncertainty is managed successfully. The following intervention modes are analysed within the AITL-WING-HITL framework when continued assistance is critical for A-UAVs.

No-control (supervisory) mode (Fig. 15A): it is a time where the AI can empirically be proved to be on such a high degree of superiority that the human's input may affect the task performance negatively. The involvement of HTMs is aimed to be minimised in this mode. The HTM, as a task-specific HITL, encourages the A-UAV in a non-decisive mood to take either one of the options determined by the vehicle itself or a different predetermined option.

Co-activity (shared-control) mode (Fig. 15B): Some tasks may not be achieved by allocating sub-task responsibilities distinctively between the HTM and A-UAVs, which may lead to compromising task performance. Combining human and robot skills via intelligent interfaces seems very appealing; in this manner, establishing principled co-activity methods to seamlessly blend the control between the human and the robot to enable the combined system to surpass both the robot and human performance with reduced human effort is a prime goal for robotics [45]. This mode assists both intelligent agents – HITL HTM and AITL AI – in achieving the common goal safely.

Collaboration (joint-control or traded control) mode (Fig. 15C): Allocated/assigned series of fine-grained sub-tasks need to be performed individually either by the AITL or HITL agent. Neither the HTM is in full control of the A-UAV nor the A-UAV is in full control of itself, where various specific sub-tasks are allocated between the HTM and A-UAV beforehand. The control is traded back and forth to execute fine-granular sub-tasks, enabling joint problem-solving. Partial control can be mainly used for tightly coupled coordination between collocated HTM and A-UAVs to achieve joint task performance, wherever difficulty that cannot be coped with by the autonomy is alerted. Instead of a supervisor dictating to a subordinate, the human and the robot engage in dialogue to exchange ideas and resolve differences in the collaborative mode [23]. This mode aims to produce a better outcome than either the human or A-UAV performs alone.

Full-control (master–slave) mode (Fig. 15D): Complete task may need to be performed by the HTM alone under extreme conditions in this mode. The HTM, as a leading agent, takes over the control and leads the A-UAV as a follower agent. Different from the collaboration mode, the A-UAV, piloted remotely by the HTM, obeys the manoeuvres performed by the HTM under any circumstances.

Cooperation (all togetherness) mode Swarms of A-UAVs sometimes need to interact with each other to accomplish a single task faster than a single A-UAV or to solve difficult tasks that are beyond a single A-UAV's capability, where each A-UAV assists in the accomplishment of the desired goal, considering its specific capabilities, e.g. carrying a very heavy payload together with a robotic arm or a suspended cable grasped by a fixed gripper, search and rescue by assigning different target Region of Interest (RoI) to multiple A-UAVs.

The main distinctive features of the intervention modes are summarised in Table 5. A merge of these intervention modes can be employed by switching from one mode to another for specific parts of a complicated task to cope with highly difficult challenges. Switching decisions between modes can be determined based on the characteristics and dominance of the modes as presented in Table 6. For instance, the switching decision for "from no-control to co-activity and then to collaboration and then to full-control and then again back to no-control" is controlled and carried out by A-UAV, HTM, HTM and "HTM & A-UAV together" respectively.

3.2.2. Modules, techniques, & interface of AITL-WING-HITL

The main components of the AITL-WING-HITL platform (Fig. 2) are already explained in the related sections of this paper above in Sections Section 3.1.1, 3.1.2, 3.1.3, and 3.1.4. Therefore, we will be focusing on the particular characteristics of the platform in this section to reveal the specific features that are gained from the mould of the aforementioned components. A-UAVs have diverse characteristics, and they are designed with particular features and onboard equipment concerning the missions they are expected to perform [7]. In this regard, the manipulation of different types of A-UAVs requires particular control parameters representing the particular features of A-UAVs. The HTM can manipulate the speed, altitude, and heading of A-UAVs, considering the other aerial vehicles in the environment both to avoid

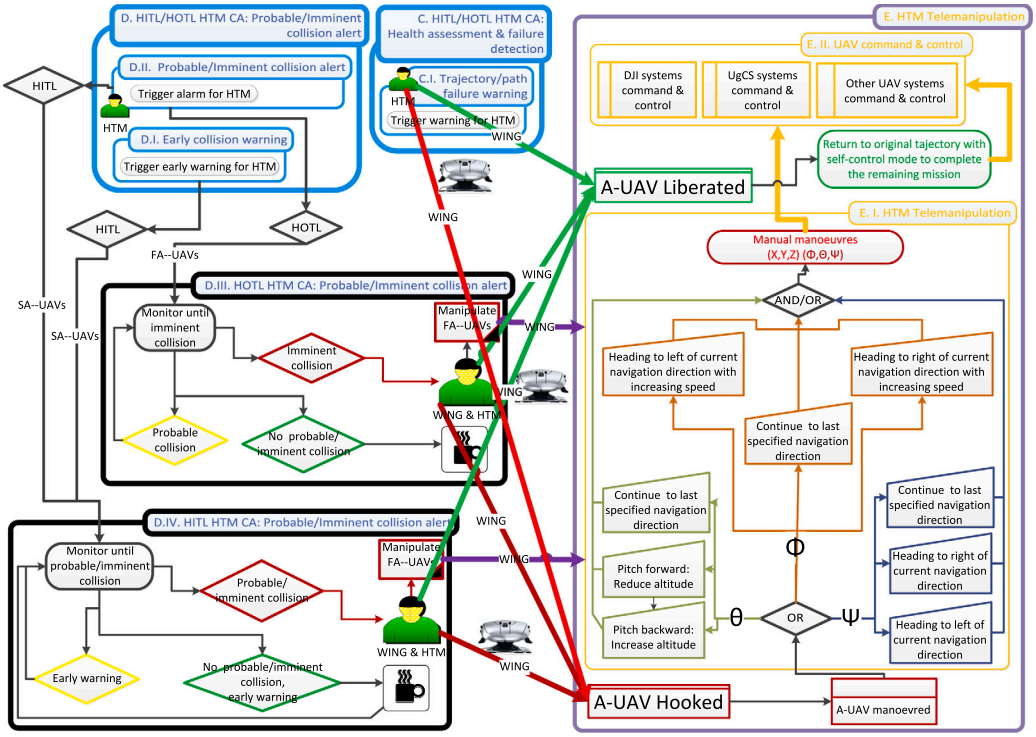

Fig. 16. Methodology of hooking and manipulation of A-UAVs using the WING. The part human intervention, D.1 (Algorithm 1), in this figure is replaced with the autonomous intervention part, D.1, in the DACM system in Supplement III (Fig. 2) when A-UAVs are manipulated by HTMs with the inputs from C.III (HOTL) and C.IV (HITL) (Algorithm 1). (For interpretation of the references to colour in this figure legend, the reader is referred to the web version of this article.)

Fig. 17. Interface of the AITL-WING-HITL platform. (For interpretation of the references to colour in this figure legend, the reader is referred to the web version of this article.)

instant collisions and not to cause new collision risks with the generated manoeuvres as illustrated in Fig. 16E.1. Commands generated through the WING are transformed to the hooked A-UAVs using the off-the-shelf drone controlling systems such as UgCS, DJI (Fig. 16E.2.) as elaborated in our previous research in [42].

Interface of the AITL-WING-HITL platform: The AITL-WING-HITL application provides an improved, easy-to-use Graphical User Interface (GUI) for manipulating A-UAVs in the specified aerial zone using the WING, leading to fine-granular force, direction, and amplitude. The interfaces of intelligent systems are supposed to be considered to reduce the cognitive load to the possible minimum complexity, paving the way for effective human intervention with a high degree of perception. In this direction, the interface of AITL-WING-HITL was designed to be as simple as possible by avoiding HTMs with unnecessary overwhelming information. Additionally, it, as displayed in Fig. 17, provides HTMs with effective perception capabilities which allow HTMs to focus on the particular sections of the interface with which they are supposed to interact. For instance, the colour of an A-UAV's heading line turns black when that UAV is suggested to the HTM to be hooked and manipulated during a collision risk. The circles of $PCTZone$ and $ICTZone$ turn

black to show that the A-UAV is hooked by the HTM for manipulation. The primary interface elements are (i) DTs of aerial traffic, (ii) the WING that is coupled between HTMs and A-UAVs within DTs, (iii) the interactive interface control elements and (iv) informative elements. Either the HITL agent or the AITL agent determines the intervention mode and transitions between these modes as outlined in Table 6. Either with a button click on the WING or with a selection from the interactive interface control elements, the HTM can switch between the interaction states (i.e. HOTL and HITL) and the intervention modes, namely, no-control (supervisory), co-activity (shared-control), collaboration (joint-control), full-control (master–slave), and cooperation (all togetherness) (Fig. 15).

Hooking with WING (Fig. 16***C.1, D.III, D.IV):*** HTMs may need to intervene in the current actions of A-UAVs for better task performance or to avoid hazards. The flights that indicate a collision risk are highlighted in the interface, and the system turns into HITL state from HOTL state. A HTM can hook one of these flights using the immersive device to manipulate its actions. The interface may suggest that a specific A-UAV shall be hooked and manipulated during a collision risk by turning its heading line black. More specifically, the system can recommend a specific A-UAV to be hooked if there is a collision risk between that A-UAV and Manned Aerial Vehicles (MAVs), where there is no possibility to hook MAVs. Similarly, fixed-wing drones are recommended by the system against rotary-wing drones, while the battery constraint feature of rotary-wing drones is evident. In the same manner, the fixed-wing drone with a stronger battery level is advised over the other fixed-wing drone with a lower battery level, whereas rotary-wing drones with stronger battery levels are proposed against other rotary-wing drones with lower battery levels. Moreover, drones with an air-based mission against drones with a ground-based mission are selected by the system for hooking, where drones with air-based missions are not required to turn to their leaving point at the original trajectory. Likewise, the slower drone can be recommended against the faster one, while the manoeuvring may be easier with the slower drone. The circles of the $PCTZone$ and $ICTZone$ turn black to denote that the A-UAV is hooked by the HTM for manipulation.

The hooking of a specific A-UAV takes place when the WING-Button-1-clicked point is within the $ICTZone$ of the A-UAV. The HTM remains in the manipulation mode until the hooking is released using the WING-Button-2-clicked point in the same way. The $ICTZone$, $PCTZone$, and the heading turn into black colour (Fig. 17) to signify the hooked A-UAVs during the manipulation phase. The HTM can hook and manipulate multiple A-UAVs simultaneously. While an A-UAV is implementing the last command in the hooked state, e.g. heading to a new direction with a new altitude, the HTM can hook other A-UAVs to manipulate their actions. In this way, multiple A-UAVs can be hooked, which means that they no longer implement their preplanned waypoints, velocity, and altitude while the WING is actively manipulating another drone. The actuation per A-UAV is performed using one of the intervention modes (Fig. 15) explained in Section 3.2.1. The liberated A-UAVs from the hooking state return to their original trajectory using the shortest path to implement their pre-planned missions.

Manipulation of A-UAVs with WING (Fig. 16***E.1):*** The mobile Internet with low-latency and high bandwidth capabilities, enabling access to information on an anywhere-anytime basis, has democratised our life in many aspects, in particular, providing fast remote operation abilities [8]. Telepresence of HTMs within aerial traffic is provided by the AITL-WING-HITL platform. The WING offers an intuitive way of controlling multiple degrees of freedom (i.e. multiple axes) simultaneously, aiming at using the human motor system effectively with a higher information capacity. One hand is in manipulating A-UAVs; the other hand is free to operate aircraft systems through the keyboard or the control panel of the AITL-WING-HITL platform. The mapping of the values acquired from the WING to drone manoeuvres is shown in Algorithm 1. This mapping actuates the hooked A-UAVs appropriately as illustrated in Fig. 16E.1. The user can choose the proper intervention mode within the interface and can translate the inputs of the WING into a particular transfer function that manipulates A-UAVs accordingly. HTMs are immersed with A-UAVs through force/torque applied or released to the rotational orientations — roll (Φ), pitch (Θ) and yaw (Ψ) channels (Fig. 4). The buttons on the WING are employed to switch between several states and actuation functions. The use of the buttons in hooking and releasing A-UAVs is explained earlier.

The SSA of aerial traffic is constantly generated using the global SSA strategy implemented by the PilotAware system (Section 3.1.3). The movements of aerial vehicles are computed by the DACM (Section 3.1.4). The DACM triggers alarms and warnings when the AITL agent experiences a difficult situation or there is a hazard, such as impending collision risks, beforehand for the HTM to take action and manipulate A-UAVs remotely. The HTM within the UTM+ATM system is authorised to intervene in the autonomous actions of A-UAVs. The HTM can adjust the position (longitudinal and lateral), altitude, angular velocity and orientation of A-UAVs concerning their environments with a quick response using the WING. It is worth emphasising that drones can be manipulated with desired navigational actions, considering the dynamic characteristics of the aerial environment and the particular drone physics-based rules defined in the system, such as manoeuvrability, velocity, and acceleration. In this sense, interactions between HTMs and A-UAVs differ depending on the capabilities of A-UAVs. For instance, a drone can accelerate to its maximum allowable speed, but not above it, even if it is forced to a velocity that is above the maximum defined speed. The discrete microstructure values of 6DoF $(x, v, z, \Psi, \Theta, \Phi)$ (Fig. 5), corresponding to the geospatial orthogonal axes (i.e. three state variables — translational coordinates (x, v, z) and rotational coordinates (Ψ, Θ, Φ), are mapped to the manoeuvrers of A-UAVs. The translational coordinates are very much dependent on the angular coordinates in our model as formulated in Algorithm 1. Taking this into consideration, the maximum manoeuvrability of the A-UAVs is determined according to the yaw, pitch and roll orientation as $(-\pi \leqslant \Psi \leqslant \pi)$, $(-\pi/2 \leqslant \Theta \leqslant \pi/2)$, and $(-\pi/2 \leqslant \Phi \leqslant \pi/2)$. The A-UAV changes its trajectory as the HTM applies the desired force on the WING. The A-UAV follows the latest action taken by the HTM if the HTM releases the force completely. In other words, the A-UAV follows the heading with specified altitude and velocity directed by the HTM, even though the WING leaves the drone for manipulating other A-UAVs for the sake of simplicity, assuming that the HTM is not required to hold the WING actions at a specific trajectory for a specific drone. In this way, multiple A-UAVs can be hooked simultaneously. The A-UAV follows similar actions continuously, where the HTM applies the maximum allowed force on the device. For instance, the heading can change to the left or right of the original direction by 15°, which results in a circular trajectory. The relationship between the inputs and outputs is managed by mapping interactions' inputs to desired outcomes concerning the particular manoeuvrability capabilities of each A-UAV. The number of actions in the specified direction (i.e. roll (Φ), pitch (Θ) and yaw (Ψ)) executed by an A-UAV, leading to the change of rotation angles of the X, Y, and Z axis is dependent on the DoF, the number of sequences executed by the HTM and their values and timestamps (e.g. Table 2, Figs. 6, 7). The hooked drone has to co-work with the HTM by following the actions directed by the HTM to increase its task performance and avoid hazardous situations. The platform reacts to any imminent collision risk. An imminent collision risk can be caused if any required desired action is not actuated by the HTM within the early warning zone (Fig. 10) and the $PcRz$ (Fig. 11) despite the system collision warnings and alarms, which may lead to making drones meet in the $IcRz$ (Fig. 12). An imminent collision risk can also be caused by the instant actions of the HTM during the implementation of any intervention modes. The WING has a significant degree of inertia, which may cause the HTM to overshoot their desired location or move too fast. To avoid unexpected manoeuvres based on the fast-changing microstructure of the WING with a sequence of multiple sub-movements, the directions of the selected intervention mode

Algorithm 1: Manipulation of A-UAVs (Fig. 16E.1) using the WING device.

Data: System input: Ψ_{Pmax} & Ψ_{Pmin} & Ψ_{Smax} & Ψ_{Smin} & Φ_{Pmax} & Φ_{Pmin} & Φ_{Pmax} & Φ_{Pmin} & Θ_{Fmax} & Θ_{Fmin} & Θ_{Bmax} & Θ_{Bmin} (Table 3)
Data: Instant input: $Ro1$.flights.Data
Result: $D_H.\Psi$ & $D_H.\Phi$ & $D_H.\Theta$ & D_H.heading & D_H.speed & D_H.alt
=> Create the hooked drone for manipulation & initialise variables;
HookedDrone D_H = new HookedDrone(); D_H = meD;
Φ_{prev} = 0; Θ_{prev}= 0; Ψ_{prev} = 0;$D_H.\Phi$ = 0; $D_H.\Theta$ = 0; $D_H.\Psi$ = 0;
=> Inputs from WING;
while *hooked* **do**
  if $((W_s == "RotationZ")\&\&((D_H.\Psi > -\pi)||(D_H.\Psi < \pi)))$ **then**
    => Assign the WING value to Yaw (Ψ);
    Ψ_{cur} = W_{val};
    if $(((\Psi_{cur} < \Psi_{Pmax})\&\&(\Psi_{cur} < \Psi_{prev}))||(\Psi_{cur} == \Psi_{Pmin}))$ **then**
      => Heading to left of the current navigation direction;
      D_H.heading = D_H.heading - $D_H.property(\Psi_{DiffDeg})$;
      $D_H.\Psi = D_H.\Psi$ - $D_H.property(\Psi_{DiffDeg})$;
    else if $(((\Psi_{cur} > \Psi_{Pmin})\&\&(\Psi_{cur} > \Psi_{prev}))||(\Psi_{cur} == \Psi_{Pmax}))$ **then**
      => Heading to right of the current navigation direction;
      D_H.heading = D_H.heading + $D_H.property(\Psi_{DiffDeg})$;
      $D_H.\Psi = D_H.\Psi$ + $D_H.property(\Psi_{DiffDeg})$;
    else
      => Continue to last specified navigation direction;
    end
    navigateD_H ($D_H.\Psi$, $D_H.\Phi$, $D_H.\Theta$, D_H.heading, D_H.speed, D_H.alt);
    Ψ_{prev} = Ψ_{cur};
  else if $((W_s == "X")\&\&((W_{val} < \Phi_{Smax})||(W_{val} > \Phi_{Pmin}))\&\&((D_H.\Phi > -\pi/2)||(D_H.\Phi < \pi/2)))$ **then**
    => Assign the WING value to Roll (Φ);
    Ψ_{cur} = W_{val};
    if $(((\Phi_{cur} < \Phi_{Smax})\&\&(\Phi_{cur} < \Phi_{prev}))||(\Phi_{cur} == \Phi_{Smin}))$ **then**
      => Roll starboard: Heading to left of current navigation direction with increasing speed;
      D_H.heading = D_H.heading - $D_H.property(\Phi_{DiffDeg})$;
      D_H.speed = D_H.speed + $D_H.property(\Phi_{DiffDeg})$;
      $D_H.\Phi = D_H.\Phi$ - $D_H.property(\Phi_{DiffDeg})$;
    else if $(((\Phi_{cur} > \Phi_{Pmin})\&\&(\Phi_{cur} > \Phi_{prev}))||(\Phi_{cur} == \Phi_{Pmax}))$ **then**
      => Roll port: Heading to right of current navigation direction with increasing speed;
      D_H.heading = D_H.heading + D_H.property(headDiff);
      D_H.speed = D_H.speed + D_H.property(speedDiff);
      $D_H.\Phi = D_H.\Phi$ + $D_H.property(\Phi_{DiffDeg})$;
    else
      => Continue to last specified navigation direction;
    end
    navigateD_H ($D_H.\Psi$, $D_H.\Phi$, $D_H.\Theta$, D_H.heading, D_H.speed, D_H.alt);
    Φ_{prev} = Φ_{cur};
  else if $((W_s == "Y")\&\&((W_{val} < \Theta_{Fmax})||(W_{val} > \Theta_{Bmin}))\&\&((D_H.\Theta > -\pi/2)||(D_H.\Theta < \pi/2)))$ **then**
    => Assign the WING value to pitch (Θ);
    Ψ_{cur} = W_{val};
    if $(((\Theta_{cur} < \Theta_{Fmax})\&\&(\Theta_{cur} < \Theta_{prev}))||(\Theta_{cur} == \Theta_{Fmin}))$ **then**
      => Pitch forward: Reduce altitude;
      D_H.alt = D_H.alt - D_H.property(altDiff);
      D_H.speed = D_H.speed - D_H.property(speedDiff);
      $D_H.\Theta = D_H.\Theta$ - $D_H.property(\Theta_{DiffDeg})$;
    else if $(((\Theta_{cur} > \Theta_{Bmin})\&\&(\Theta_{cur} > \Theta_{prev}))||(\Theta_{cur} == \Theta_{Bmax}))$ **then**
      => Pitch backward: Increase altitude;
      D_H.alt = D_H.alt + D_H.property(altDiff);
      D_H.speed = D_H.speed - D_H.property(speedDiff);
      $D_H.\Theta = D_H.\Theta$ + $D_H.property(\Theta_{DiffDeg})$;
    else
      => Continue to last specified navigation direction;
    end
    navigateD_H ($D_H.\Psi$, $D_H.\Phi$, $D_H.\Theta$, D_H.heading, D_H.speed, D_H.alt); Θ_{prev} = Θ_{cur};
  else
    => Return to original trajectory after released from hooking;
    hooked = "false";
    ReturnToOriginalTrajectory();
  end
end

within 6DoF are taken into consideration along with the capabilities of the drones in manipulation. This provides the user with the means to limit movement with more resistance.

A HTM can be cautioned with an alert by the AITL AI agent about the emerging situation. Telemanipulation requests and intervention requirements can be prioritised by the HTM or the system, and several of these can be commanded to take an idle safe position or trajectory (e.g. a circular trajectory as mentioned above) without endangering the vehicle itself and surrounding traffic by hooking multiple A-UAVs simultaneously. They can be handled later in priority scheduling order or hazard states (i.e. red, yellow, green) by a HTM, enabling task allocation. This property enables a single HTM with limited sensorimotor capabilities to manage a large area with heavy aerial traffic.

Liberation of A-UAVs and their return to the original trajectory (Fig. 16***C.1, D.III, D.IV):*** A specific drone can be released from hooking when the WING-Button-2-clicked point is within the $ICTZone$ of the A-UAV. The circles denoting $ICTZone$, $PCTZone$, and the heading line turn into their original colour from black (Fig. 17) after the A-UAV is liberated to indicate that they are performing their tasks independently with the AITL agent themselves. A-UAVs orient themselves in Euclidean space by means of the preplanned trajectory after being released from

the hook, considering their physical manoeuvring features and the instant SSA environmental inputs.

4. Experimental design

The developed platform – AITL-WING-HITL – needs to be assessed first in the environment of a simulation, then in the drone containment cage, and finally in real-field environments to ensure that the targeted objectives are achieved. The performance of humans while teleoperating multiple A-UAVs using the WING, as well as the functions of the platform, was evaluated in the simulation module of the developed platform. Volunteers were needed to test the developed platform for an hour, which aims to investigate further advancements through scenario-based experiments to improve the techniques and approaches before real-world tests. The AITL-WING-HITL platform, with simulation capabilities (Supplement III (Fig. 2, G.1)), provides an easy way to establish varying scenarios with multiple A-UAVs with their particular routes. One HTM can manipulate multiple drones using one WING in a one-to-many intervention mode. We would like to measure if the HTM can adjust their hand impedance sufficiently — application of hand force and releasing of the force (i.e. the translated input force into sub-movement microstructure states in Supplement I: Yaw (Tables I, II, Figs. 1, 2) and Roll (Tables III, IV, Figs. 3, 4) and Pitch (Tables V, VII, Figs. 5, 6) channels) at the desired time intervals to trigger the targeted actuation. Several scenarios were generated to measure (i) the capability of the user in adapting to the dynamically scaling DT environments and (ii) the efficiency of the responses to different scenarios using the WING with the various intervention modes (Fig. 15). HTMs are expected to improve their skills in real-world implementations as they immerse themselves in the platform over time, using the relation between the amplitude of the mouse movement, which is based on the force applied in channels, and the observed actuation displayed on the interface.

4.1. Policies followed before, during and after the experiment

Participation in the experiments was entirely voluntary, and participants were free to withdraw from the study at any time without providing a reason. No personally identifiable information was recorded, and all data were fully anonymised. Participants granted permission for the experimenter to access anonymised system-generated data and anonymised questionnaires completed during the study. Individuals with diagnosed chronic conditions (e.g. epilepsy) were not permitted to participate. Participants were informed that the anonymised data would be used for research purposes and shared with the academic community through publications. All data will be securely stored and protected for the next seven years in accordance with ethical guidelines (Section 10).

4.2. Environmental settings

University staff and students were voluntarily registered for the evaluation of the AITL-WING-HITL platform through some designed scenarios. An individual's designated code, age and sex information were recorded; no other personal information was registered. The demographics of participants are shown in Supplement-V (the third column of Table 1). The age ranges from 19 to 55. No volunteer came forward from the female gender group, where the number of females is significantly less than the number of males gender in the School of Engineering and Computing from which most of the participants volunteered. The participants are grouped into sub-classes as experienced staff, non-experienced staff, experienced students and non-experienced students as displayed in Supplement-V (the second column of Table 1) based on the second and third questions in the Overall Quality Questionnaire (OQQ) (Supplement IV Table 2). The participants who both answered the second question as "e" (>20) and the third question as "c" (<5 years) or "d" (<10 years) or "e" (>10 years) were grouped as experienced. 4 staff out of 11 and 7 students out of 12 were tagged as experienced (Supplement-V (Table 1)). These sub-groups were incorporated into the analysis of the platform, in particular, the evaluation of the WING's capacity to manipulate A-UAVs, which concerns other close-range aerial vehicles, for the purpose of mitigating collision risks. It is noteworthy to emphasise that discomfort could arise during the non-stop, long test of 6 experimental episodes, and one objective was to measure the emerging discomfort. All participants knew that they could quit the test at any time they wished. Alternatively, the test can be ended by the mentor at any time. In this respect, 3 participants decided to withdraw from the experiment in the middle of the experiment, and the mentor decided to stop the experiment for one of the volunteers due to increasing tension. These volunteers were excluded from the experiment, and no data from these volunteers were included in the assessment of this report. The user-friendly application provides a co-simulation environment coupling real and simulated A-UAVs. Manipulating co-simulated A-UAVs is carried out using the aerial DT interface that is integrated with the WING to avoid the risk of collisions by allowing the user to readily respond to developing situations regarding all other manned or unmanned flights in the environment. The simulation interface makes it easier to repeat the same experiments.

The experimental episodes conducted in this simulated environment were designed to: (i) analyse participants' task performance; (ii) enhance immersive navigation experiences using the WING system to accelerate task performance through human sensorimotor adaptation – where human perception continuously recalibrates in response to new inputs; and (iii) assess Simulation and Cyber Sickness (SCS) symptoms prior to real-world field tests, in order to identify mitigation strategies that improve the functionality of the AITL-WING-HITL platform. Participants were required to complete the Simulation Sickness Questionnaire (SSQ) at three stages: before the orientation training, after the orientation (but prior to the experimental episodes), and after completing all episodes. This allowed for tracking changes in physiological symptoms throughout the experiment. Additionally, they were asked to complete an Overall Quality Assessment Questionnaire (OQQ) at the end of the experiment to evaluate potential areas for further improvement. To maintain experimental continuity and minimise duration, SSQ measurements were not taken between scenarios/episodes, thereby avoiding interruptions and allowing for an uninterrupted assessment of symptom severity.

A 13-minute orientation was provided to help participants familiarise themselves with the AITL-WING-HITL platform and the WING system. Specifically, the experimental session began with a training phase. Participants first received a brief 5-minute tutorial on the interface, during which the experiment mentor demonstrated how the WING's combined functionalities could be used to control drones via the platform. Key scenarios were demonstrated to clarify the experiment's objectives – for example: "What happens if neither the human nor the system intervenes, resulting in a collision?" and "How does the platform autonomously respond to impending, probable, and imminent collision risks using a minimum deviation strategy?" Following the tutorial, participants engaged in a 7-minute practice session, supported by the experimenter. During this time, they freely explored the system's features to assess how quickly they could adapt to its functionalities. The participants were made aware that the primary objective of the experiment was to avoid collisions using the fewest possible manoeuvres and to maintain minimal deviation from the original flight paths – ensuring safe separation between drones through the WING system.

Each participant was scheduled for an episode duration of seven minutes, with the trial comprising six episodes, each designed to achieve a distinct objective. These episodes incorporated three different scenarios, with each scenario being repeated twice across the six episodes. Based on prior research, it is expected that prolonged continuous exposure can result in more severe symptoms of Simulation

Sickness (SS) compared to multiple shorter exposures [46]. Specifically, as observed by Kennedy et al. [47], two key temporal phenomena are associated with SS: the severity of symptoms tends to increase with longer exposure durations during a single session, while repeated exposure to simulation over time can lead to adaptation, reducing symptom severity [46]. To explore these dynamics, the experiment was designed as a continuous, long trial with no breaks between episodes, which may heighten participants' susceptibility to SS if symptoms occur. Each participant completed the full trial in approximately 55 min – comprising a 13-minute orientation followed by six episodes of seven minutes each ($6 \times 7 = 42$ min). If a participant failed an episode (e.g. by causing a collision), the episode was repeated, extending the total trial duration by an additional seven minutes. Although environmental settings remained constant across episode repetitions, participants were instructed to avoid collision risks using different features of the WING system, each involving distinct intervention modes (Fig. 15). Participants could control multiple drones at risk of collision, with capabilities such as altering and locking navigational direction, forcing drones to hover in a safe location, or instructing them to orbit a defined geospatial point until released. All drone movements and granular actuation data were tracked and recorded for later analysis, allowing assessment of both precision and consistency across trials. Participants received real-time warnings upon detection of imminent collision risks. In such cases, the system automatically transitioned from the HOTL state to the HITL state to enable immediate human intervention.

The experiment designed in this study aims to assess both participants' task performance and the unpleasant symptoms experienced during the sessions. Researchers and developers utilising flight simulators or DT technologies must remain mindful of SCS, as it can negatively affect experimental outcomes. Consequently, before widespread adoption, all VR technologies should be rigorously tested for their potential to induce discomfort in users [46]. Analysing the symptoms associated with SCS in relation to specific user interactions within the application can inform system enhancements that may significantly reduce symptom severity. To establish a baseline, participants were assessed prior to the experiment to capture any pre-existing symptoms. This is critical, as individuals can exhibit considerable variability in their tolerance to environmental changes, necessitating pre- and post-test comparisons to determine statistically significant differences. Additionally, a questionnaire (i.e. OQQ), consisting of both Likert-scale and open-ended questions, was administered to evaluate the current functionality of the system and to identify areas for further improvement regarding user experience and task performance. The full questionnaire is provided in the supplementary materials (Supplement IV, Table 2). To measure the severity of SS symptoms, the widely adopted SSQ developed by Kennedy et al. [47] was used. SCS is a syndrome similar to motion sickness, often encountered in simulator or immersive environments, akin to what sailors experience at sea [48]. The SSQ includes 16 symptoms (listed in Supplement IV, Table 1) and primarily captures physiological discomfort and autonomic nervous system activation. Each symptom in the SSQ is rated on a four-point scale: 0 (“none”), 1 (“slight”), 2 (“moderate”), and 3 (“severe”). The symptoms are categorised into three subscales – Nausea (N), Oculomotor Disturbances (O), and Disorientation (D) – as well as an overall Total Severity Score (TS). Some symptoms contribute to multiple subscales; for instance, “Difficulty focusing” is included in both the “oculomotor” and “disorientation” categories. Subscale scores are calculated by summing the symptom ratings within each category and multiplying by particular weights: 9.54 for Nausea (range: 0–200.34), 13.92 for Disorientation (range: 0–292.32), and 7.58 for Oculomotor Disturbance (range: 0–159.18). Rather than a simple sum of raw scores, this weighted scoring system, constructed by Kennedy et al. [47], offers a more accurate and nuanced measure of overall SCS, as it accounts for the varying severity levels across its three subscales. The total symptom score is obtained by summing all 16 symptom ratings and multiplying the result by 3.74, yielding an overall SSQ score ranging from 0 to 179.52.

4.3. Test in simulation

The experimental test began with a training session. Participants were first provided with a concise 5-minute tutorial on the interface. The experiment mentor then demonstrated how the 6DoF functionalities of the WING system could be employed to control A-UAVs via the AITL-WING-HITL platform. Two key scenarios were demonstrated to clarify the experiment's objectives: (1) what occurs when neither the human operator nor the system intervenes, resulting in a collision; and (2) how the AITL-WING-HITL platform autonomously responds to impending, probable, and imminent collision risks using a minimum-deviation strategy. These scenarios were illustrated using two 7-minute recorded videos, “01_No-intervention-no-CA.wmv” and “02_No-intervention-with-CA.wmv”, available in [49]. Following the demonstration, participants engaged in a 7-minute hands-on practice session with support from the experimenter. During this session, they freely explored the platform's functionalities to assess how quickly they could adapt. It was emphasised that the primary objective throughout the episodes was to avoid collisions using the fewest possible manoeuvres via the WING system. In essence, participants were expected to complete each CA task by safely and minimally deviating from the original flight path. Participants were instructed to execute CA manoeuvres outside the ICTZone for safety, but as close as possible to it for efficiency — ideally within the PCTZone. They were also required to avoid creating any new collision risks with other nearby aerial vehicles while evading imminent collisions. A collision during any episode was considered a failure, requiring the participant to repeat that episode without interruption. Three challenging collision-avoidance tasks were assigned, each involving potential conflicts with other aerial vehicles. These three scenarios were repeated once, resulting in a total of six episodes. The repetition allowed for measuring user progress between the first and second attempts. Once participants were familiarised with all system setups, the independent experimental sessions were conducted. Participants were fully immersed in a simulated aerial environment through the WING interface. Given that latency in visual feedback can significantly impair haptic task performance [50,51], our application provided real-time visual updates of both the WING's actions and the environmental interactions (SSA) with other flights. This ensured high transparency, enabling users to properly immerse themselves in the remote environment and promptly correct any undesirable actions. Each participant completed the six episodes over 42 min, as previously described. For four participants, the test duration increased by seven minutes due to episode failures requiring repetition: two participants from the non-experienced student group in Episode 3, one from the non-experienced staff group in Episode 3, and one from the experienced staff group in Episode 5. All system-generated data produced by participants during the simulation were recorded for subsequent performance evaluation and statistical comparison.

Each participant was able to visually interact with specific A-UAVs and manipulate their navigation and trajectories in relation to nearby flights, with the goal of successfully completing the task without collisions and maximising task performance. All participants began with the first episode and proceeded sequentially through the second, third, fourth, fifth, and sixth episodes without interruption. The experiment concluded with the completion of post-test questionnaires. Upon finishing all six episodes, participants were asked to complete the SSQ and a function-specific evaluation – the OQQ – as previously described. These instruments were used to assess overall user experience and system effectiveness from multiple perspectives. In addition to the questionnaire data, system-generated records from each episode were analysed to evaluate both individual participant performance and overall system functionality. These records included: (i) the time taken to successfully complete each episode (e.g. time required for the HTM to resolve specific problems); (ii) the deviation distance from the original planned trajectory; and (iii) the number of failures, such as imminent collision alarms or actual collisions. The following sections provide detailed elaboration of the scenarios used in the experiment.

Table 7
Statistical significance test of deviation comparisons using one-tailed dependent T-test for paired samples: Comparison of the episodes within the scenarios to conclude if the learning, improvement and adaptation are statistically significant.

Scenario	Episode	Average dev diff (metre)	# of improvement	Sample size (n)	Average of differences	Significance level (α):	SD of differences	*P*-value		Statistical significance	Fig.
I	I–II	−2314	18	23	−100.6087	0.01	126.7706	0.0009667	$p < 0.01$	Significant	18(a)
II	III–IV	−633	14	23	−27.5217	0.01	183.5751	0.4797	$p > 0.01$	NOT significant	18(b)
III	V–VI	−813	13	23	−35.3478	0.01	176.0255	0.346	$p > 0.01$	NOT significant	18(c)

4.3.1. The first scenario within the first two episodes

The platform's autonomous response to imminent collision risks using a minimum deviation strategy was demonstrated in the video titled "02_No-intervention-with-CA.wmv". Participants were expected to replicate similar manoeuvres during the first two episodes, specifically within the PCTZone. Entering the ICTZone significantly increases the risk of collision and is considered a weakness in participant performance. Any actual collision was classified as a failure, requiring the repetition of the episode. Upon entering the PCTZone, participants had a window of 3 s to reach the ICTZone, and up to 6 s before a collision would occur if no corrective action was taken. Participant performance was evaluated by comparing their manoeuvres to both the system's benchmark trajectory demonstrated in "02_No-intervention-with-CA.wmv" and to one another, primarily based on the deviation from the original flight path. To ensure the measurement of participants' unassisted performance, the full-control (master–slave) intervention mode (Fig. 15) was employed. This configuration prevents the system from initiating any autonomous manoeuvres during imminent collision risks or actual collisions. Thus, the assessment reflects purely the participants' capabilities without system interference. For an illustrative example of the manoeuvres expected in the first two episodes, readers are referred to the video titled "FirstScenario.wmv" in [49].

4.3.2. The second scenario within the third and fourth episodes

In this scenario, the co-activity (shared) intervention mode (Fig. 15) was employed. Participants were expected to perform vertical manoeuvres – either upward or downward – based on the altitudes and velocities of nearby flights posing collision risks. Entering the ICTZone significantly increases the likelihood of a collision, and if the system triggers an autonomous manoeuvre to avoid an imminent collision, the episode is considered a failure and must be repeated. Participants had a 3-second window to reach the ICTZone after entering the PCTZone, within which autonomous interventions are activated. Participant performance was evaluated by comparing their trajectories to the system's benchmark manoeuvre (i.e. "02_No-intervention-with-CA.wmv"), as well as against one another, with particular attention to the deviation from the original trajectory.

4.3.3. The third scenario within the last two episodes

In the third and fourth episodes, participants were expected to perform directional manoeuvres opposite to the detected threat: ascending when the potential collision path involved a descending trajectory, and descending when the collision threat came from below. The co-activity (shared) intervention mode (Fig. 15) was employed for this scenario. Entering the ICTZone significantly increased the risk of collision, and any autonomous manoeuvre initiated by the system to prevent an imminent collision was considered a failure, requiring the episode to be repeated. Upon entering the PCTZone, participants had a 3-second window to respond before the ICTZone threshold was reached and autonomous actions were triggered. Participant performance was assessed by comparing their manoeuvres against the system's benchmark (i.e. "02_No-intervention-with-CA.wmv") and against one another, with a focus on the deviation from the original flight trajectory.

5. Experimental results

A dependent t-test for paired samples was conducted to evaluate the outcomes of the quantitative data collected during the experiment. The analysis was performed with a statistical significance level corresponding to a 99% confidence interval. A detailed summary of the experimental results is provided in Supplement V to facilitate further analysis and enable researchers to draw broader conclusions. The key findings from these results are outlined below.

5.1. Results: System-generated recordings

The summarised deviation results, autonomously recorded by the system during the experiments, are presented in Supplement V (Table 1). As shown in Table 7, which presents averaged data from Figs. 18(a), 18(b), and 18(c), Scenario I demonstrates a statistically significant improvement from Episode I to Episode II. In contrast, Scenarios II (Episodes III to IV) and III (Episodes V to VI) exhibit only minor, statistically insignificant improvements (i.e. 28 m and 35 m, respectively). A total of 18 out of 23 participants improved their performance in Scenario I, whereas only 14 participants improved in Scenarios II and III. This suggests that Scenarios II and III may require additional training for participants to achieve more substantial performance gains. These scenarios likely impose a higher cognitive load, as they demand greater attention to the real-time Situation Awareness (SA) and navigation data generated by the system. This increased demand may be attributed in part to the cognitive limitations associated with interpreting such information via the 2D GUI of the AITL-WING-HITL platform. Fig. 18(d) visualises the average deviation across all scenarios and episodes relative to the benchmark value – the Minimum Expected Deviation Level (MEDL) – recorded in the autonomous mode (i.e. 730 m). This visualisation highlights the relative differences in performance, both between participants and in comparison with the autonomous system. Participant performance is considered more favourable the closer the deviation is to the MEDL. Participant adaptation appears to be more effective in Scenario I, with the deviation in Episode II decreasing to 837 m – approaching the MEDL – likely due to the reduced cognitive load. In Episode I of Scenario I, where participants first began engaging with the WING and the interface, the deviation was higher (938 m), which is expected due to the initial learning curve. In comparison, the first episodes of Scenarios II and III yielded slightly smaller deviations (920 m and 924 m, respectively), likely due to prior exposure. However, subsequent improvements in Scenarios II and III were minimal (892 m and 889 m, respectively), indicating that additional exposure alone may not be sufficient for significant performance enhancement in tasks involving greater cognitive complexity.

From a broader perspective, the classification of average deviation values across participant groups is visualised in Fig. 19, based on the detailed data provided in Supplement V (Table 1). The group-specific analyses are summarised below:

– Scenario I: All participant groups demonstrated performance improvements from Episode I to Episode II, with respective improvement values of 30 m, 172 m, 108 m, and 47 m. While it was expected that the expert group would perform best when engaging with the

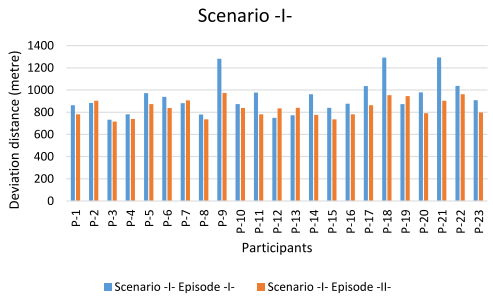

(a) Results for the first scenario: Improvement for 18 participants.

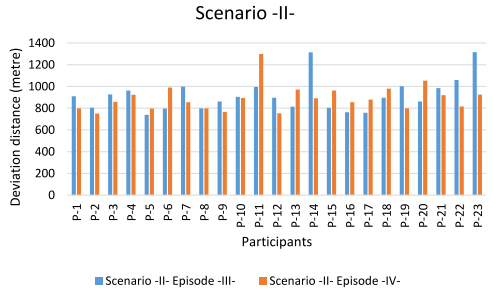

(b) Results for the second scenario: Improvement for 14 participants.

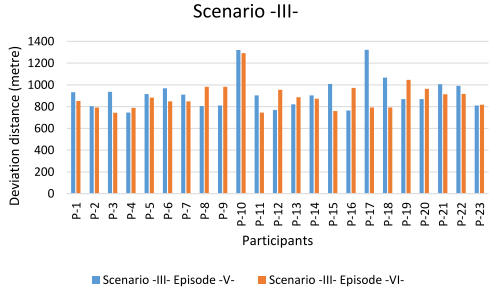

(c) Results for the third scenario: Improvement for 14 participants.

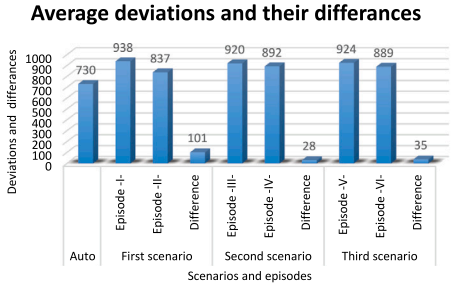

(d) Average results of the scenarios per participant (Figs. 18a, 18b, 18c). "Auto" indicates the minimum expected deviation level (MEDL) that is executed by the autonomous mode to avoid collision risks.

Fig. 18. Graphical presentation of the results obtained from the scenarios elaborated in Supplement-V (Table 1).

WING platform, the results indicate that both prior experience and familiarity with similar systems play a significant role in enhancing performance. The experienced staff group outperformed the others, achieving deviation values of 815 m in Episode I and 785 m in Episode II. Notably, the non-experienced staff showed the greatest improvement, reducing their deviation by 172 m. It is important to note that achieving improvements becomes increasingly difficult as performance approaches the MEDL, due to the elevated risk of collision. In this context, the experienced staff's relatively modest improvement of 30 m is reasonable. Interestingly, the non-experienced students performed better than the experienced students, with deviation values of 840 m and 793 m, compared to 957 m and 849 m, respectively.

– Scenario II: All groups, with the exception of the experienced students (–44 m), improved their performance from Episode III to Episode IV, with improvement values of 68 m, 73 m, and 32 m. Although the experienced students initially outperformed the other groups with a deviation of 870 m in Episode III, their performance declined in Episode IV, with a deviation of 940 m. In contrast, the non-experienced staff again achieved the highest improvement (73 m), demonstrating consistent learning and adaptation.

– Scenario III: All groups improved their performance from Episode V to Episode VI, except for the non-experienced student group, which showed a performance decline (–36 m). The most notable improvement was again observed in the non-experienced staff group, with a deviation reduction of 99 m. The experienced staff group maintained the best overall performance, with deviations of 854 m in Episode V and 794 m in Episode VI, while the non-experienced staff demonstrated the largest performance gain in this scenario.

5.2. Results: Simulation sickness questionnaire

The computation of SSQ scores based on reported symptoms is detailed in Supplement IV (Table 1). While some studies (e.g. [52–54]) suggest that the severity of SS symptoms increases over time, others (e.g. [55]) argue that symptoms tend to decrease with continued interaction with the system. Given these conflicting findings, the detailed SSQ results from this study are provided in Supplement V (Table 2). Fig. 20 presents the overall SSQ summary scores, including the TS and subscale scores. The total SS score increased from 38.38 at the beginning of the experiment to 42.93 after the training phase, and further to 53.5 by the end of the experiment. The increase from the start to the training phase was not statistically significant, whereas the increase from the training phase to the completion of all scenarios was significant ($p < 0.01$). Nausea (N) and Oculomotor (O) scores showed a slight, statistically insignificant decrease following the training phase and a slight, statistically insignificant increase by the end of the experiment ($p > 0.01$ in both cases). In contrast, Disorientation (D) scores showed a consistent and statistically significant increase across all three phases, rising from 62.34 at the beginning to 68.99 after training and reaching 93.20 by the end of the experiment ($p < 0.01$). It is important to note that even at the final measurement, the disorientation scores remained well below the maximum possible value of 292.32 (as shown in Supplement IV, Table 1).

Participant group SSQ scores are illustrated in Fig. 21, where symptoms – Nausea (N), Oculomotor (O), and Disorientation (D) – are combined to compare differences across groups, and in Fig. 22, where scores are grouped by experimental phase (start, training, and end) to highlight trends per symptom. As shown in Fig. 21, there was no noticeable increase in SSQ scores for the experienced staff across the experiment phases (i.e. 28.99, 26.18, 28.05). In contrast, a consistent and significant increase was observed for both the non-experienced staff (i.e. 37.4, 49.15, 58.77) and non-experienced students (i.e. 44.88, 50.12, 61.34) from the beginning to the end of the experiment. Although the training phase was designed to alleviate simulator sickness symptoms, it instead resulted in a significant increase in scores for the non-experienced staff (49.15) and non-experienced students (50.12). In contrast, the decrease in SSQ scores for the experienced staff (26.18) and experienced students (41.14) during the training phase was not statistically significant. Among all groups, the experienced staff consistently reported the lowest SS levels. In Fig. 22, while the experienced

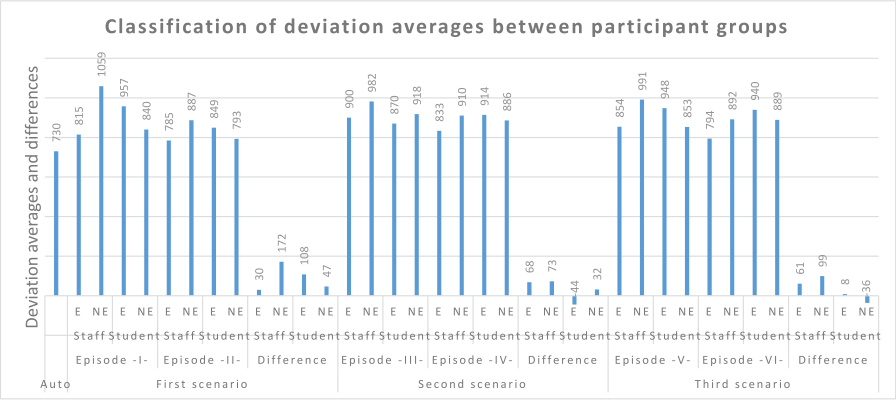

Fig. 19. Classification of deviation averages between participant groups (Supplement-V (Table 1)).

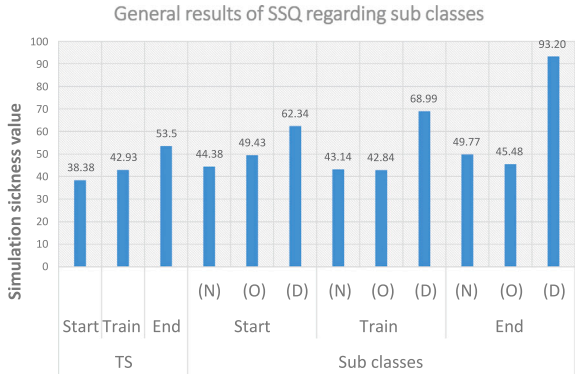

Fig. 20. General scores of the SSQ regarding total SS (TS) and sub class syndromes (Supplement IV (Table 1)).

staff did not show a significant increase in total SSQ scores over time, the disorientation (D) subscale did increase significantly – from 38.28 to 45.24 – during the experiment. This increase is masked in the overall total due to decreases in the (N) and (O) subscales, which dropped to 16.69 and 24.63, respectively, compared to their initial values (N: 23.85, O: 37.9). The (D) symptom increased significantly across all participant groups. The (N) subscale decreased significantly for the experienced staff but increased for all other groups except the experienced students. The (O) subscale decreased significantly for the experienced staff and both student groups, but increased for the non-experienced staff from the start to the end of the experiment.

5.3. Results: Overall quality questionnaire

The OQQ is provided in Supplement IV (Table 2). Detailed results obtained from the OQQ are presented in Supplement V and summarised in Fig. 23 by question order, in Fig. 24 by score ranking, and in Fig. 25 by participant subgroup. The overall average score across all questionnaire items is 3.9 out of 5. Question Q-5 (“Manoeuvring left/right is easy to implement with the WING”) received the highest approval rating, with an average score of 4.7. In contrast, question Q-16 (“I found the overall AITL-WING-HITL interface as well as the WING easy to use and scalable to support a single HTM controlling more than one A-UAV synchronously”) received the lowest score, averaging 3.4. Questions Q-5, Q-12, Q-11, Q-10, Q-4, and Q-13 were all rated highly, each scoring above 4 out of 5. Regarding participant subgroups (Fig. 25), the experienced staff group provided the highest overall rating, with an average score of 4.29. Conversely, the non-experienced student group gave the lowest ratings, with an average score of 3.67. The non-experienced staff and experienced student groups gave similar ratings (3.90 and 3.88, respectively). Notably, the experienced staff group scored highest across all questionnaire categories. The immersive capabilities of the WING in simulation environments were found to be highly effective. Participants reported that the AITL-WING-HITL platform, in conjunction with the WING, met most of their expectations in manipulating A-UAVs. The responsiveness of the A-UAVs was considered highly satisfactory, particularly in terms of translating the WING’s discrete microstructural inputs into desired task-oriented outputs — such as trajectory adjustments, manoeuvres, velocity, altitude, and heading. Overall, participants responded positively to remote manipulation of A-UAVs in scenarios involving pending, probable, or imminent collision risks using the WING’s 6DoF functionality. Notably, 16 out of 23 participants – 7 of whom were experienced – expressed a preference for using the WING over traditional joysticks (Q-24 in Supplement V, Table 3). QoE can be assessed through measurable QoS parameters; a decline in QoS typically results in reduced QoE [56]. In this context, the immersive quality, comfort, and overall usability of the AITL-WING-HITL platform and the integrated WING were all rated highly. No significant effects of system latency were observed on task performance or responsiveness, indicating a high level of transparency in the simulation environment and, consequently, a high QoE. Based on participant feedback, the primary concerns and additional features to be considered for future integration into the system are outlined as follows.

– Executing manoeuvres above or below other vehicles requires close attention to real-time flight parameters – especially altitude – since discerning vertical separation between vehicles can be challenging in the platform’s 2D interactive interface (Fig. 17). This is particularly problematic when aircraft converge at similar latitude and longitude coordinates.

– Experienced participants, familiar with 3D simulation environments, recommended the development of a 3D visualisation mode for the platform to enhance spatial awareness.

– Manipulating vehicle trajectories along the Z-axis using the WING could be made more intuitive and functional, particularly when discrete altitude changes are needed – especially in the downward (Z-negative) direction of the device.

– The platform could assist users by suggesting optimal manoeuvring actions (e.g. “descend 50 m”, “turn 15° left”) based on real-time SSA and nearby aircraft data, as it already does for scenarios involving probable or imminent collision risks. Such features may help reduce cognitive load.

6. Challenges

(i) Latencies in wireless communication between A-UAVs and HTMs are a clear limitation, hindering the development of highly transparent DT systems. From a broader perspective, time-varying delays are inevitable during collaborative operations – arising from communication

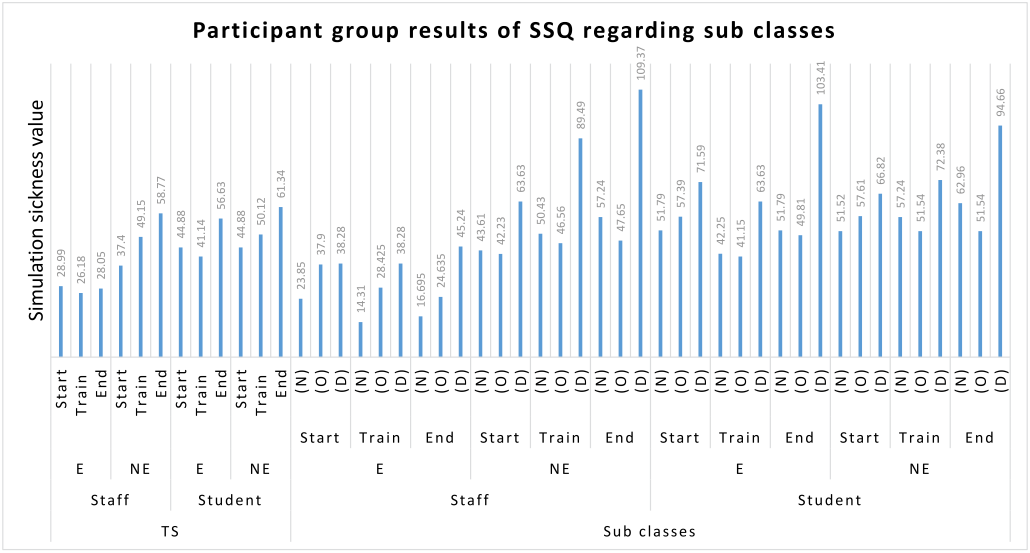

Fig. 21. Participant group scores of SSQ regarding total SS (TS) and SS results with sub classes (Supplement V (Table 2)). The symptoms ((N), (O), (D)) are brought together to perceive the difference from each other.

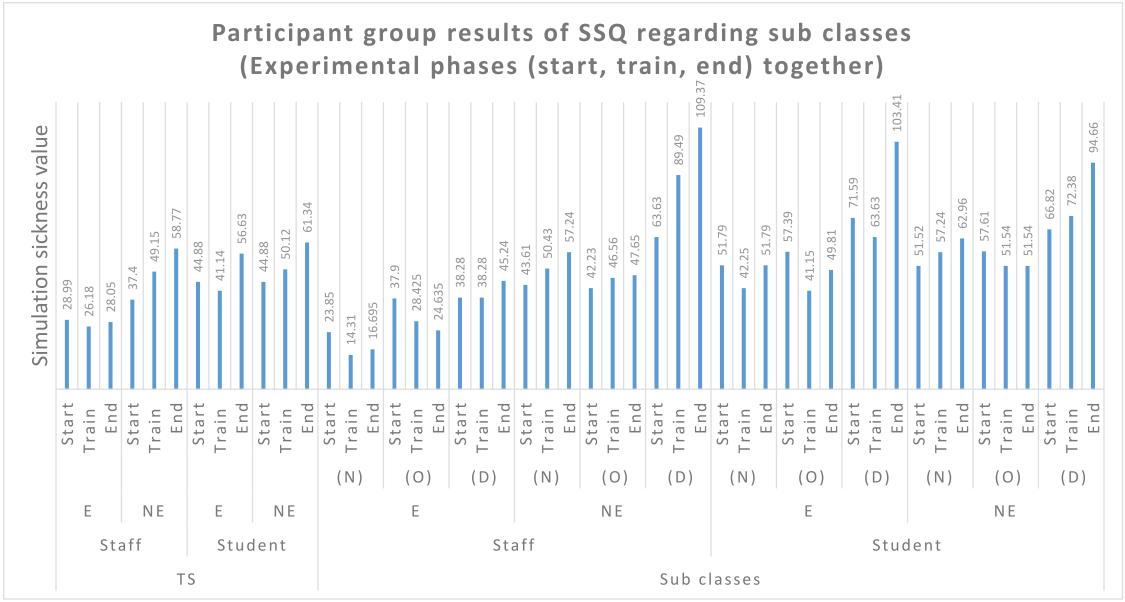

Fig. 22. Participant group scores of SSQ regarding total SS (TS) and SS results with sub classes (Supplement V (Table 2)). Experimental phases (start, train, end) are brought together to perceive the trend per symptom.

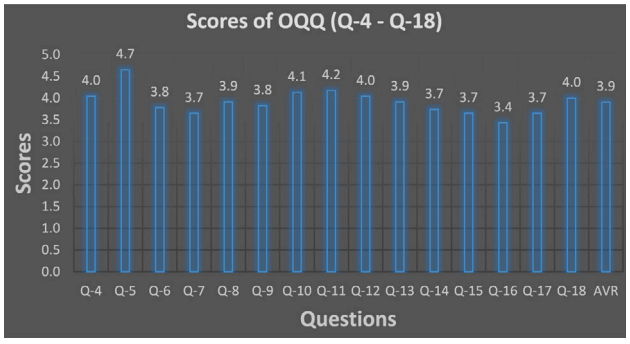

Fig. 23. Scores of OQQ (Q-4 - Q-18) (Supplement V (Table 3)).

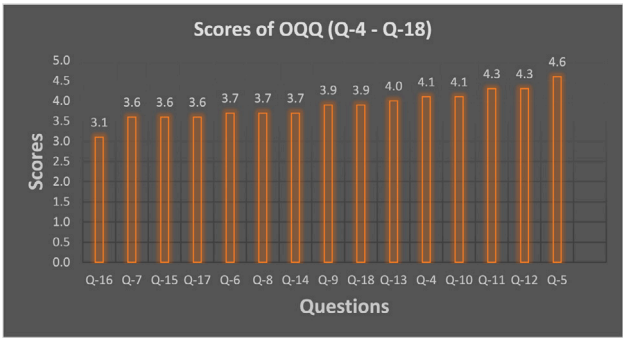

Fig. 24. Sorted scores of OQQ (Q-4 – Q-18) (Supplement V (Table 3)).

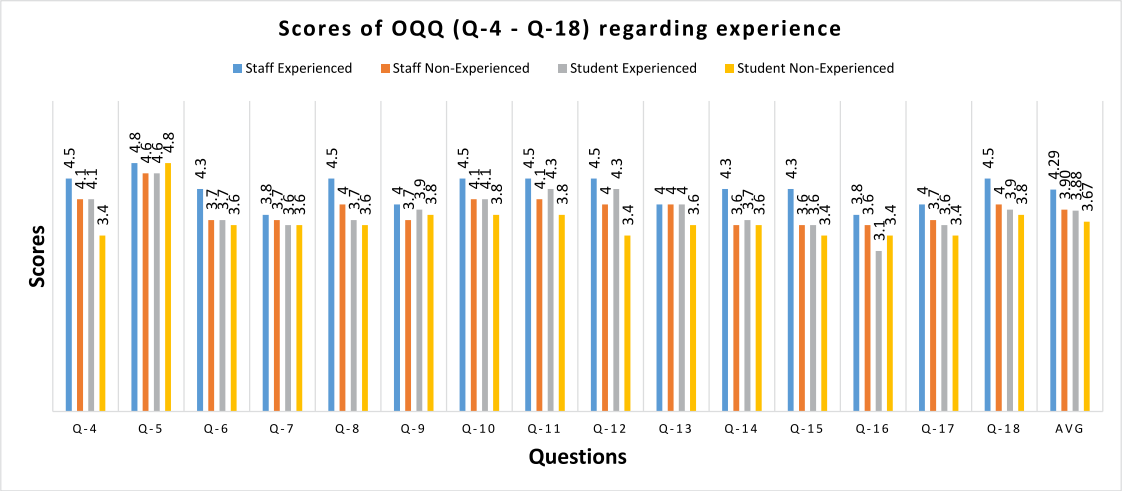

Fig. 25. Scores of OQQ (Q-4–Q-18) (Supplement V (Table 3)) regarding participant sub-groups.

lag, decision-making delays affecting the QoE of HTMs, the processing of large volumes of sensor data, and actuation delays. To enable effective telemanipulation of aerial robots – especially for CA – it is essential to develop transparent systems equipped with estimation-based predictive displays and directional aids (Figs. 9,10) that compensate for these latencies. Further studies on transparent systems, in particular, building the transparency standards, such as IEEE Std 7001-2021 [57], are of prime importance, considering the autonomous systems.

(ii) Malicious interference poses significant threat. A nearby radio transmitter can readily initiate a denial-of-service attack – e.g. via jamming – with reaction times on the order of tens of microseconds, significantly increasing packet loss rates in Vehicle-to-Vehicle (V2V) communication, as demonstrated in multiple studies [58–60]. Additionally, false data injections may occur, highlighting the need for robust authentication mechanisms to validate all inputs [7]. Given these risks, cybersecurity must be treated as a primary concern well in advance of the widespread deployment of telemanipulated A-UAV systems.

(iii) Determining optimal obstacle-free trajectories for drones is a complex challenge, constrained by factors such as airspace structure, communication coverage, battery limitations, collision risk, and terrain avoidance [61]. All these constraints must be thoroughly considered in the design of telemanipulation approaches for A-UAV platforms.

7. Lessons learned

(i) 3D interface development for DT systems – excluding extraneous information – can substantially reduce cognitive load during telemanipulation, enhancing operator effectiveness and situational awareness.

(ii) Even with high-quality SA information, effective human telemanipulation remains highly dependent on the cognitive, perceptual, and motor abilities of HTMs, including spatial orientation skills [8]. To mitigate risks from erroneous decisions, it is critical to leverage local intelligence (i.e. AITL) at the remote site (Fig. 15).

(iii) Many drone operations can benefit from a unified framework that facilitates coordinated access to integrated airspace and efficient routing to task locations [62]. The development of robust telemanipulation platforms, as investigated in this study, supports the realisation of such frameworks.

(iv) A major challenge in non-fault-tolerant and non-delay-tolerant telemanipulation of AVs lies in the requirement for real-time intervention with high perceptual awareness and minimal latency (i.e. rapid action-response capability) [8]. A human–teleoperator interface with low cognitive demand can streamline interaction and ensure compatibility with real-world AV capabilities [8]. Future systems must incorporate advanced, safety-critical interface functionalities, supported by cutting-edge communication infrastructure and analytical tools, to enable tight, time-sensitive coupling between the cyber domain of HTMs and the physical domain of AVs [8]. This research focused on developing such a platform – designed to reduce cognitive load and support one-to-many A-UAV telemanipulation – by leveraging high-functionality coupling tools like the WING and interfaces such as AITL-WING-HITL.

8. Discussion

FA-UAVs are expected to execute their missions with minimal to no human intervention. However, in complex, real-world environments – particularly when multiple UAV missions are conducted by various organisations within a shared, integrated aerospace alongside manned aircraft – unforeseen situations may arise that exceed the autonomous capabilities of A-UAVs. The integration of A-UAVs into broader traffic management systems necessitates the use of coordinated platforms that support collective movement, ensuring safe and efficient mission execution while mitigating mid-air collision risks, as detailed in [42]. Such platforms foster the necessary cohesion to maintain safe separation distances between aerial vehicles. The HOTL and HITL paradigms remain vital in the operation of AVs. Despite decades of research and recent advancements by the tech industry and academia, significant gaps persist in AV capabilities [63]. Addressing unexpected issues remotely, through vehicle teleoperation (i.e. remote driving, manipulation, or control), is therefore critical — both for ensuring public safety and mitigating potential cybersecurity threats [8]. This research aimed to develop an integrated, collaborative approach that enables humans and intelligent drones to co-work in resolving operational challenges (e.g. CA, mission-specific task execution). The proposed platform – AITL-WING-HITL – was designed to provide HTMs with comprehensive monitoring of aerial traffic and direct manipulation capabilities over A-UAVs through advanced intervention tools. Central to this platform is the WING – a force-sensitive, precision control device that facilitates immersive, multi-modal interaction. By enabling a high level of synergistic collaboration between human operators and A-UAVs, the WING ensures effective task execution through an intelligent and responsive interface.

The AITL-WING-HITL platform was evaluated through participant testing using measurable parameters to identify areas for further improvement in the developed interface and techniques, as outlined in Section 4. The outcomes – derived from system-generated recordings, Kennedy's SSQ, and the OQQ – are presented in Section 5, supported by figures, tables, and detailed analyses of group performances. Overall,

participants found the platform easy to use, particularly highlighting the high functionality of the WING. This conclusion is based on participant feedback, analysis of user experiences, and preliminary quantitative results gathered during the experimental sessions. While two participants expressed dissatisfaction with the placement of certain interface elements, efficient interactions were generally observed when using the WING. Participants were able to generate trajectories closely aligned with the ideal data set (i.e. MEDL), which was created by the AITL system as a benchmark based on the most optimal trajectories. These results support the conclusion that the trajectory data sets produced by participants using the WING are efficient, and that users can collaboratively and coactively telemanipulate A-UAVs to achieve near-optimal mission outcomes using this intuitive and deployable device. Furthermore, the trajectory waypoints, speeds, and azimuth angles obtained from AITL–HITL co-activity highlight the WING's ease of implementation and manipulation in a practical and effective manner. Additionally, four participants remarked that a wireless version of the WING would enhance user immersion by allowing more freedom of movement within the DT environments of aerial traffic.

The experimental results validate the effectiveness of the proposed AITL-WING-HITL architecture. The WING enables HTMs to perform omnidirectional control in telemanipulating A-UAVs. By combining translational and rotational movements, the WING facilitates the generation of multiple DoFs and functions, allowing users to accomplish highly complex tasks through varied input combinations. The framework, with its robust capabilities, is scalable to accommodate multiple A-UAVs operating within mixed aerial traffic environments. Through its immersive system design and synchronous communication features, AITL-WING-HITL enables a single HTM to simultaneously manipulate multiple A-UAVs, even under uncertain, unstructured, and dynamic conditions. This research demonstrates that the proposed framework enhances HTM effectiveness by integrating AITL and HITL co-activity, supporting a wide range of automated, user-friendly functions alongside high-fidelity telepresence and telemanipulation capabilities. Moreover, the results indicate that most participants adapted to the platform with ease, requiring minimal training. The AITL-WING-HITL system is highly flexible, addressing the complex, multidimensional dynamics inherent in A-UAV operations. However, based on the analysis of results from Scenarios II and III – compared to Scenario I – participants' perceptual accuracy showed a slight decline due to increased cognitive load. This was particularly evident when generating manoeuvring trajectories that required flying over or under other vehicles, where altitude differences were difficult to perceive in the platform's 2D interactive environment. These findings highlight the potential benefits of 3D telemanipulation interfaces in enhancing the spatial awareness of HTMs. Accordingly, the integration of 3D visual content is identified as a key direction for future development (Section 10). Overall, the experimental design and findings presented in this study offer valuable insights for researchers and developers engaged in similar efforts within the field of remote aerial vehicle manipulation.

9. Limitations of the system

Changes in heart rate, respiration rate, and central nervous system activity are key physiological indicators associated with SCS. Therefore, automatically monitoring these parameters – such as through Electroencephalography (EEG) and Electrocardiography (ECG) – could provide a more comprehensive and objective assessment. This approach may offer deeper insights into the onset and progression of SCS symptoms, potentially yielding more accurate and less biased results compared to self-reports. Numerous studies, including those by Dumaska et al. [46], have demonstrated a strong correlation between these physiological indicators and SCS. Additionally, the participant pool in our study comprised 23 individuals – 7 short of our target of 30 – which limited the breadth of our evaluation. Nonetheless, the results obtained from the experiment offered meaningful insights and demonstrated statistical significance in key findings.

10. Conclusion and future work

This research investigates the collaboration between human cognition and machine intelligence through the development of a synergistic collective platform – AITL-WING-HITL – which integrates several subsystems into a unified architecture (Fig. 2). This architecture generates DTs of aerial traffic and incorporates an immersive control device – the WING (Section 3.1.1) – to enable HTMs to seamlessly interact with and manipulate A-UAVs within mixed aerial traffic environments. The AITL-WING-HITL platform allows HTMs to switch between: (i) intervention modes, ranging from no-control (supervisory) to full-control (master–slave) teleoperation (Fig. 15), and (ii) motion modes, including translational motion (x, υ, z) and rotational orientation (Ψ, Θ, Φ) (Fig. 4), depending on the required manipulation task. Using the WING with 6DoF, the platform enables the remote extension of human expertise, offering HTMs the ability to telemanipulate A-UAVs with a high degree of precision and flexibility across various intervention modes. This capability supports: (i) achieving high levels of task performance, and (ii) ensuring that A-UAVs exhibit reliable autonomous behaviour under unanticipated conditions – both critical for maintaining aerial and ground safety. The system was evaluated in a range of simulated laboratory scenarios involving both experienced and inexperienced participants to assess platform functionality and the effectiveness of the WING in telemanipulating A-UAVs. Results indicate that teleimpedance manipulation via the WING is effective: participants were able to modulate hand impedance appropriately – that is, applying and releasing hand forces with precise timing – to perform the required actuation tasks successfully. The key outcomes of this research are summarised as follows:

– The WING, integrated within the AITL-WING-HITL platform, provides HTMs with finely tuned, tightly coupled control of A-UAVs by translating its discrete microstructural signals directly into task-oriented actions with high responsiveness.

– The WING's dexterous force-generation capability, combined with strong spatial, cognitive, and ergonomic features and minimal training requirements, enables efficient centralised telemanipulation of decentralised A-UAVs within the AITL-WING-HITL architecture, resulting in high task performance.

– The co-work and co-activity mechanisms between HTMs and A-UAVs, facilitated through the platform's intervention modes – investigated here for the first time specifically in the context of A-UAVs – enable synergistic collaboration. This dual-intelligence system leverages both vehicle-side autonomy and human-side decision-making to achieve complex operational goals through effective human–machine dialogue.

– This research advances the understanding of A-UAV telemanipulation by exploring user immersion and adaptability within the AITL-WING-HITL framework. It provides valuable insights into how A-UAVs can be safely and efficiently manipulated – especially when the autonomous system (AITL agent), acting as the new "driver", encounters situations that exceed its autonomous capabilities.

Scalable systems such as AITL-WING-HITL offer a viable solution to the current limitations of A-UAV usage, enabling their integration into a wide range of applications without having to wait for the perfection of autonomous technologies – a milestone still years away. In the future, complex, time- and safety-critical real-world tasks will be performed coactively by HTMs and AITL-enabled A-UAVs. To enhance HTM perception and cognitive engagement, the current 2D GUI of the AITL-WING-HITL platform is planned to be replaced with a more immersive 3D visual environment. Additionally, key questions remain for future investigation: What is the optimal number of A-UAVs that a single highly skilled HTM can effectively manage? And how many HTMs should be assigned to a given region, city, or country, taking into account factors such as aerial traffic density, A-UAV automation levels, and task-specific assistance needs? These assessments aim to ensure the safe and efficient operation of aerospace systems within an

integrated UTM+ATM framework. Another important future direction is the use of reinforcement learning (RL) – including Transfer Learning (TL) [64] and Federated Learning (FL) [65] – to train drones based on insights gained during HTM-led telemanipulation. This approach will help A-UAVs acquire greater autonomy by learning how to act under uncertain conditions. In the long term, our objective is to develop robust systems in which HTMs and A-UAVs collaborate seamlessly to accomplish complex tasks with high levels of performance.

CRediT authorship contribution statement

Kaya Kuru: Writing – review & editing, Writing – original draft, Visualization, Validation, Supervision, Software, Resources, Project administration, Methodology, Investigation, Funding acquisition, Formal analysis, Data curation, Conceptualization. **Sam Worthington:** Writing – review & editing, Validation, Resources. **Darren Ansell:** Validation, Supervision, Resources, Investigation, Funding acquisition. **John M. Pinder:** Writing – review & editing, Resources, Investigation, Formal analysis. **Aadithya Sujit:** Writing – review & editing, Resources, Investigation. **Benjamin J. Watkinson:** Writing – review & editing, Validation, Resources, Formal analysis. **Keith Vinning:** Writing – review & editing, Resources, Investigation, Data curation. **Lee Moore:** Writing – review & editing, Resources, Data curation. **Chris Gilbert:** Writing – review & editing, Resources, Formal analysis. **David Jones:** Writing – review & editing, Validation, Resources, Investigation. **Claire Tinker-Mill:** Writing – review & editing, Validation, Supervision, Project administration, Funding acquisition.

Declaration of competing interest

The authors declare that they have no known competing financial interests or personal relationships that could have appeared to influence the work reported in this paper.

Funding, ethics and acknowledgements

This report presents independent research funded by the European Regional Development Fund's (ERDF) business support programme (Project Number: 19R19P03775). The funding agreement guaranteed the authors full independence in the design of the study, data interpretation, and the writing and publication of this report. The views expressed herein are those of the authors and do not necessarily reflect those of the funder. This research was conducted with ethical approval from the University of Lancashire (Science Ethics Review Panel Reference: SCIENCE 01031). The authors extend their sincere thanks to all participants who volunteered for the experiment, as well as to the anonymous reviewers for their valuable feedback and constructive suggestions.

Appendix A. Supplementary data

Supplementary material related to this article can be found online at https://doi.org/10.1016/j.robot.2026.105486.

Data availability

Data will be made available on request.

References

[1] NewYorkTimes, A successful exhibition of electrical transmission without wires in the garden, 1898.
[2] T.K. Sarkar, R. Mailloux, A.A. Oliner, M. Salazar-Palma, D.L. Sengupta, History of Wireless, Wiley, NJ, USA, 2006.
[3] N. Tesla, Method of and apparatus for controlling mechanism of moving vessels or vehicles, 1898, U.S. Patent US613809A.
[4] J. Turi, Tesla's toy boat: A drone before its time, 2014.
[5] K. Kuru, D. Ansell, W. Khan, H. Yetgin, Analysis and optimization of unmanned aerial vehicle swarms in logistics: An intelligent delivery platform, IEEE Access 7 (2019) 15804–15831, http://dx.doi.org/10.1109/ACCESS.2019.2892716.
[6] K. Kuru, W. Khan, A framework for the synergistic integration of fully autonomous ground vehicles with smart city, IEEE Access 9 (2021) 923–948, http://dx.doi.org/10.1109/ACCESS.2020.3046999.
[7] K. Kuru, Planning the future of smart cities with swarms of fully autonomous unmanned aerial vehicles using a novel framework, IEEE Access 9 (2021) 6571–6595, http://dx.doi.org/10.1109/ACCESS.2020.3049094.
[8] K. Kuru, Conceptualisation of human-on-the-loop haptic teleoperation with fully autonomous self-driving vehicles in the urban environment, IEEE Open J. Intell. Transp. Syst. 2 (2021) 448–469, http://dx.doi.org/10.1109/OJITS.2021.3132725.
[9] J.M. Bradshaw, V. Dignum, C. Jonker, M. Sierhuis, Human-agent-robot teamwork, IEEE Intell. Syst. 27 (2) (2012) 8–13, http://dx.doi.org/10.1109/MIS.2012.37.
[10] M. Chowdhury, M. Maier, Toward dynamic hart-centric task offloading over fiwi infrastructures in the tactile internet era, IEEE Commun. Mag. 57 (11) (2019) 123–128, http://dx.doi.org/10.1109/MCOM.001.1800669.
[11] Y. Li, Trends in control and decision-making for human–robot collaboration systems [bookshelf], IEEE Control Syst. Mag. 39 (2) (2019) 101–103, http://dx.doi.org/10.1109/MCS.2018.2888714.
[12] M. Shahbazi, S.F. Atashzar, R.V. Patel, A systematic review of multilateral teleoperation systems, IEEE Trans. Haptics 11 (3) (2018) 338–356, http://dx.doi.org/10.1109/TOH.2018.2818134.
[13] W.R. Ferrell, T.B. Sheridan, Supervisory control of remote manipulation, IEEE Spectr. 4 (10) (1967) 81–88, http://dx.doi.org/10.1109/MSPEC.1967.5217126.
[14] K. Kuru, Trustfsdv: Framework for building and maintaining trust in self-driving vehicles, IEEE Access 10 (2022) 82814–82833, http://dx.doi.org/10.1109/ACCESS.2022.3196941.
[15] V.R. Garate, S. Gholami, A. Ajoudani, A scalable framework for multi-robot tele-impedance control, IEEE Trans. Robotics 37 (6) (2021) 2052–2066, http://dx.doi.org/10.1109/TRO.2021.3071530.
[16] Y. Nakauchi, T. Okada, N. Yamasaki, Y. Anzai, Multi-agent interface architecture for human–robot cooperation, in: Proceedings 1992 IEEE International Conference on Robotics and Automation, Vol. 3, 1992, pp. 2786–2788, http://dx.doi.org/10.1109/ROBOT.1992.220012.
[17] T. Laengle, T. Hoeniger, L. Zhu, Cooperation in human–robot-teams, in: ISIE'97 Proceeding of the IEEE International Symposium on Industrial Electronics, Vol. 3, 1997, pp. 1297–1301, http://dx.doi.org/10.1109/ISIE.1997.648935.
[18] T. Suzuki, K. Yokota, H. Asama, H. Kaetsu, I. Endo, Cooperation between the human operator and the multi-agent robotic system: evaluation of agent monitoring methods for the human interface system, in: Proceedings 1995 IEEE/RSJ International Conference on Intelligent Robots and Systems. Human Robot Interaction and Cooperative Robots, Vol. 1, 1995, pp. 206–211, http://dx.doi.org/10.1109/IROS.1995.525798, vol.1.
[19] T. Fujita, H. Kimura, The design of software development system for multiple robots, in: Proceedings of 1993 IEEE/RSJ International Conference on Intelligent Robots and Systems, IROS'93, Vol. 2, 1993, pp. 1119–1125, http://dx.doi.org/10.1109/IROS.1993.583331, vol.2.
[20] T. Fong, S. Grange, C. Thorpe, C. Baur, Multi-robot remote driving with collaborative control, in: Proceedings 10th IEEE International Workshop on Robot and Human Interactive Communication. ROMAN 2001 (Cat. No. 01TH8591), 2001, pp. 237–242, http://dx.doi.org/10.1109/ROMAN.2001.981908.
[21] T. Fong, C. Thorpe, C. Baur, Multi-robot remote driving with collaborative control, IEEE Trans. Ind. Electron. 50 (4) (2003) 699–704, http://dx.doi.org/10.1109/TIE.2003.814768.
[22] T.W. Fong, C. Thorpe, C. Baur, Advanced interfaces for vehicle teleoperation: Collaborative control, sensor fusion displays, and remote driving tools, Auton. Robot.: Spec. Issue Teleoperation Interfaces 11 (1) (2001) 77–85.
[23] T.W. Fong, Collaborative Control: A Robot-Centric Model for Vehicle Teleoperation (Ph. D. thesis), Carnegie Mellon University, Pittsburgh, PA, 2001.
[24] I. Nourbakhsh, K. Sycara, M. Koes, M. Yong, M. Lewis, S. Burion, Human–robot teaming for search and rescue, IEEE Pervasive Comput. 4 (1) (2005) 72–79, http://dx.doi.org/10.1109/MPRV.2005.13.

[25] S. Hirche, M. Buss, Human-oriented control for haptic teleoperation, Proc. IEEE 100 (3) (2012) 623–647, http://dx.doi.org/10.1109/JPROC.2011.2175150.
[26] A.K. Mithal, S.A. Douglas, Differences in movement microstructure of the mouse and the finger-controlled isometric joystick, in: Proceedings of the SIGCHI Conference on Human Factors in Computing Systems, CHI'96, Association for Computing Machinery, New York, NY, USA, 1996, pp. 300–307, http://dx.doi.org/10.1145/238386.238533.
[27] M. Martins, A. Cunha, L. Morgado, Usability test of 3dconnexion 3d mice versus keyboard+mouse in second life undertaken by people with motor disabilities due to medullary lesions, Procedia Comput. Sci. 14 (2012) 119–127, http://dx.doi.org/10.1016/j.procs.2012.10.014, Proceedings of the 4th International Conference on Software Development for Enhancing Accessibility and Fighting Info-exclusion (DSAI 2012).
[28] M.J. Turner, T. Morris, M. Sandoval, 12DoF Interaction for Scientific Visualisation, in: T.R. Wan, F. Vidal (Eds.), Computer Graphics and Visual Computing, The Eurographics Association, 2017, http://dx.doi.org/10.2312/cgvc.20171274.
[29] M. Sandoval, Multiple Degrees-of-Freedom Input Devices for Interactive Command and Control Within Virtual Reality in Industrial Visualizations (Ph. D. thesis), Department of Computer Science, The University of Manchester, Manchester, UK, 2023.
[30] M. Sandoval, T. Morris, M. Turner, Controlling 3D visualisations with multiple degrees of freedom, in: F.P. Vidal, G.K.L. Tam, J.C. Roberts (Eds.), Computer Graphics and Visual Computing, CGVC, The Eurographics Association, 2019, http://dx.doi.org/10.2312/cgvc.20191263.
[31] R.A. Suárez Fernández, J.L. Sanchez-Lopez, C. Sampedro, H. Bavle, M. Molina, P. Campoy, Natural user interfaces for human-drone multi-modal interaction, in: 2016 International Conference on Unmanned Aircraft Systems, ICUAS, 2016, pp. 1013–1022, http://dx.doi.org/10.1109/ICUAS.2016.7502665.
[32] E. Peshkova, M. Hitz, B. Kaufmann, Natural interaction techniques for an unmanned aerial vehicle system, IEEE Pervasive Comput. 16 (01) (2017) 34–42, http://dx.doi.org/10.1109/MPRV.2017.3.
[33] P. Abtahi, J.L.E.D.Y. Zhao, J.A. Landay, Drone near me: Exploring touch-based human-drone interaction, Proc. ACM Interact. Mob. Wearable Ubiquitous Technol. 1 (3) (2017) http://dx.doi.org/10.1145/3130899.
[34] K. Kuru, H. Yetgin, Transformation to advanced mechatronics systems within new industrial revolution: A novel framework in automation of everything (aoe), IEEE Access 7 (2019) 41395–41415, http://dx.doi.org/10.1109/ACCESS.2019.2907809.
[35] S. Bouabdallah, M. Becker, R. Siegwart, Autonomous miniature flying robots: coming soon! - research, development, and results, IEEE Robot. Autom. Mag. 14 (3) (2007) 88–98, http://dx.doi.org/10.1109/MRA.2007.901323.
[36] G. Coppin, F. Legras, Autonomy spectrum and performance perception issues in swarm supervisory control, Proc. IEEE 100 (3) (2012) 590–603, http://dx.doi.org/10.1109/JPROC.2011.2174103.
[37] M. Radovic, Tech talk: Untangling the 5 levels of drone autonomy, 2019.
[38] K. Nonami, Present state and future prospect of autonomous control technology for industrial drones, IEEJ Trans. Electr. Electron. Eng. 15 (1) (2020) 6–11, http://dx.doi.org/10.1002/tee.23041, arXiv:https://onlinelibrary.wiley.com/doi/pdf/10.1002/tee.23041.
[39] A. Murray, J. Rhymer, D.G. Sirmon, Humans and technology: Forms of conjoined agency in organizations, Acad. Manag. Rev. 46 (3) (2021) 552–571, http://dx.doi.org/10.5465/amr.2019.0186.
[40] M. Anderson, K. Fort, Human where? a new scale defining human involvement in technology communities from an ethical standpoint, Int. Rev. Inf. Ethics 31 (1) (2022).
[41] M. Say, Loti looks at 'humans in the loop' in ai deployments, 2025.
[42] K. Kuru, J.M. Pinder, B.J. Watkinson, D. Ansell, K. Vinning, L. Moore, C. Gilbert, A. Sujit, D. Jones, Toward mid-air collision-free trajectory for autonomous and pilot-controlled unmanned aerial vehicles, IEEE Access 11 (2023) 100323–100342, http://dx.doi.org/10.1109/ACCESS.2023.3314504.
[43] R.W. Osborne, Y. Bar-Shalom, P. Willett, G. Baker, Design of an adaptive passive collision warning system for uavs, IEEE Trans. Aerosp. Electron. Syst. 47 (3) (2011) 2169–2189, http://dx.doi.org/10.1109/TAES.2011.5937290.
[44] K. Kuru, Human-in-the-loop telemanipulation schemes for autonomous unmanned aerial systems, in: 2024 4th Interdisciplinary Conference on Electrics and Computer, INTCEC, 2024, pp. 1–6, http://dx.doi.org/10.1109/INTCEC61833.2024.10603071.
[45] N. Amirshirzad, A. Kumru, E. Oztop, Human adaptation to human–robot shared control, IEEE Trans. Hum.–Mach. Syst. 49 (2) (2019) 126–136, http://dx.doi.org/10.1109/THMS.2018.2884719.
[46] N. Dużmańska, P. Strojny, A. Strojny, Can simulator sickness be avoided? A review on temporal aspects of simulator sickness, 9, 2018, http://dx.doi.org/10.3389/fpsyg.2018.02132,
[47] R.S. Kennedy, N.E. Lane, K.S. Berbaum, M.G. Lilienthal, Simulator sickness questionnaire: An enhanced method for quantifying simulator sickness, Int. J. Aviat. Psychol. 3 (3) (1993) 203–220, http://dx.doi.org/10.1207/s15327108ijap0303_3, arXiv:https://doi.org/10.1207/s15327108ijap0303_3.
[48] K. Brunnström, E. Dima, T. Qureshi, M. Johanson, M. Andersson, M. Sjöström, Latency impact on quality of experience in a virtual reality simulator for remote control of machines, Signal Process., Image Commun. 89 (2020) 116005, http://dx.doi.org/10.1016/j.image.2020.116005.
[49] K. Kuru, Telemanipulation of autonomous drones using digital twins of aerial traffic, 2024, http://dx.doi.org/10.21227/kn5m-z290.
[50] C. Jay, M. Glencross, R. Hubbold, Modeling the effects of delayed haptic and visual feedback in a collaborative virtual environment, ACM Trans. Comput.-Hum. Interact. 14 (2) (2007) 8–es, http://dx.doi.org/10.1145/1275511.1275514.
[51] C. Jay, R. Hubbold, Delayed visual and haptic feedback in a reciprocal tapping task, in: First Joint Eurohaptics Conference and Symposium on Haptic Interfaces for Virtual Environment and Teleoperator Systems. World Haptics Conference, 2005, pp. 655–656, http://dx.doi.org/10.1109/WHC.2005.29.
[52] J.D. Moss, E.R. Muth, Characteristics of head-mounted displays and their effects on simulator sickness, Hum. Factors 53 (3) (2011) 308–319, http://dx.doi.org/10.1177/0018720811405196, PMID: 21830515. arXiv:https://doi.org/10.1177/0018720811405196.
[53] B.-C. Min, S.-C. Chung, Y.-K. Min, K. Sakamoto, Psychophysiological evaluation of simulator sickness evoked by a graphic simulator, Appl. Ergon. 35 (6) (2004) 549–556, http://dx.doi.org/10.1016/j.apergo.2004.06.002.
[54] J. Lee, M. Kim, J. Kim, A study on immersion and vr sickness in walking interaction for immersive virtual reality applications, Symmetry 9 (5) (2017) http://dx.doi.org/10.3390/sym9050078.
[55] S.V.G. Cobb, S. Nichols, A. Ramsey, J.R. Wilson, Virtual reality-induced symptoms and effects (vrise), Presence: Teleoper. Virtual Env. 8 (2) (1999) 169–186, http://dx.doi.org/10.1162/105474699566152.
[56] K. Desai, S. Raghuraman, R. Jin, B. Prabhakaran, Qoe studies on interactive 3d tele-immersion, in: 2017 IEEE International Symposium on Multimedia, ISM, 2017, pp. 130–137, http://dx.doi.org/10.1109/ISM.2017.27.
[57] IEEE Standard for Transparency of Autonomous Systems, IEEE Std 7001–2021, 2022, pp. 1–54, http://dx.doi.org/10.1109/IEEESTD.2022.9726144.
[58] K. Sjoberg, P. Andres, T. Buburuzan, A. Brakemeier, Cooperative intelligent transport systems in Europe: Current deployment status and outlook, IEEE Veh. Technol. Mag. 12 (2) (2017) 89–97.
[59] N. Lyamin, A. Vinel, D. Smely, B. Bellalta, Etsi dcc: Decentralized congestion control in c-its, IEEE Commun. Mag. 56 (12) (2018) 112–118.
[60] O. Punal, C. Pereira, A. Aguiar, J. Gross, Experimental characterization and modeling of rf jamming attacks on vanets, IEEE Trans. Veh. Technol. 64 (2) (2015) 524–540.
[61] S. Sekander, H. Tabassum, E. Hossain, Multi-tier drone architecture for 5g/b5g cellular networks: Challenges and trends and prospects, IEEE Commun. Mag. 56 (3) (2018) 96–103.
[62] M. Gharibi, R. Boutaba, S.L. Waslander, Internet of drones, IEEE Access 4 (2016) 1148–1162, http://dx.doi.org/10.1109/ACCESS.2016.2537208.
[63] B. Goldfain, P. Drews, C. You, M. Barulic, O. Velev, P. Tsiotras, J.M. Rehg, Autorally: An open platform for aggressive autonomous driving, IEEE Control Syst. Mag. 39 (1) (2019) 26–55, http://dx.doi.org/10.1109/MCS.2018.2876958.
[64] K. Kuru, Definition of multi-objective deep reinforcement learning reward functions for self-driving vehicles in the urban environment, IEEE Trans. Veh. Technol. 11 (2024) 1–12.
[65] K. Kuru, Management of geo-distributed intelligence: Deep insight as a service (DINSaaS) on forged cloud platforms (FCP), J. Parallel Distrib. Comput. 149 (2021) 103–118, http://dx.doi.org/10.1016/j.jpdc.2020.11.009.

Kaya Kuru received the B.Sc. degree from National Defense University (Turkish Military Academy), the A.D.P./Major degree in Computer Engineering from Middle East Technical University (METU), the M.B.A. degree from Selcuk University, and the M.Sc. and Ph.D. degrees in Computer Science/Informatics from METU. He completed his postdoctoral studies with the School of Electronics and Computer Science, University of Southampton, U.K. He was with the IT Department of Gulhane Training and Research Hospital and the University of Health Sciences as a DBA, a SW Developer, the SW Development Manager, and the IT Manager for 15 years. He is currently a software engineer and a Professor of Artificial Intelligence. He has recently engaged in the implementation of numerous AI-based real-world projects. His research interests include the development of geo-distributed autonomous intelligent systems using FL, ML, DL, and DRL with CPSs.

Sam Worthington received a BEng and M.Sc. in Mechanical Engineering from the University of Manchester. He is a design engineer and entrepreneur with a focus on creative problem-solving supported by sound engineering principles. He is the director of Worthington Sharpe Ltd and the developer of the patented WING 3D computer input device. Experience in developing products based on new and emerging technologies, and in applying alternative approaches to design and development problems based on proven engineering principles. Industry expertise includes: HCI, subsea oil and gas industry, and UAVs.

Darren Ansell received a B.SC. from the University of Manchester Institute of Science and Technology in electrical and electronic engineering and a Ph.D. from Cranfield University in antenna optimisation using evolutionary algorithms. He is the engineering lead for Space and Aerospace and Professor in Aerospace Engineering. He previously worked in industry at BAE Systems in management roles, specialising in Mission Systems and Autonomy.

John Michael Pinder received a B.Sc. degree in AI from the University of Sunderland, an M.Sc. in Robotics and Automation and a Ph.D. degrees in Autonomous Systems from the University of Salford. He is a Data Scientist and has over 20 years of experience applying technology to solve practical problems and generate value for customers. Previously, Dr. Pinder worked for a Robotics & Automation control software company, helping medium-to large enterprises across a wide range of industrial sectors to develop bespoke automated machinery.

Aadithya Sujit received a B.Sc in Mechanical Engineering from Visvesvaraya Technological University and an M.Sc in Aerospace Engineering from Linkoping University, Sweden. He specialises in aerospace vehicle design & development and is currently supporting industries with R&D activities. He has previously worked at TU Delft in the Netherlands developing bio-inspired UAVs, prior to which he worked at National Aerospace Laboratories in India as a UAV Project Engineer.

Benjamin Jon Watkinson has an M.Sc. in Robotics Engineering from the University of Central Lancashire. He has 9 years of experience working with NASA, BAE Systems and several SMEs supporting product development activities and research. He is currently a Hardware/Flight Test integration lead. His research interests include the development of bespoke robotics systems and drone systems to solve real-world problems.

Keith Vinning, OBE, is the project lead in flight testing and development support and is a GA pilot with 50 years of flight experience. Keith received a B.Sc. Honours degree in Electrical Engineering and Telecommunications from Aston University in 1981. He gained 49 years of experience in telecommunications product and business development, holding senior roles within BT and Fujitsu in the UK and Europe. Joined PilotAware in 2015 and was awarded an OBE in 2020 for services to Aviation Safety based on the work done with PilotAware Ltd.

Lee Moore is the CEO of PilotAware Ltd. He is a software and systems lead and Pilot. 35 years in semiconductor and electronic design automation, digital ASIC design, processor design, and software design tools. Experienced in both multinational and start-up companies GEC Telecommunications, NEC Semiconductors, Synopsys Inc., Cadence Design Systems Inc.

Chris Gilbert received a B.Sc. degree from the University of Bristol in Physics. He is a Network Lead Pilot, General Manager, of Motorola Networks EMEA, CEO of wireless network start-ups in Silicon Valley and the UK, Director of a chip company and two security companies and PilotAware Ltd.

David Jones received A' Levels degree from St. Austin's Academy in Economics, Maths, and Physics. He is a professional freelance videographer and chief drone pilot providing services in filmmaking and surveying with PfCO. His background in outdoor sports helps a lot when it comes to working with adventure companies that want to create amazing videos to help their own advertising and marketing.

Claire Louisa Tinker-Mill received a B.Sc. degree in Biological Sciences with Biomedicine, an M.Sc. degree in Biomedicine and a Ph.D. degree in Biophysics from Lancaster University. Previously, Dr. Claire worked as a Project Manager at Lancaster University. She managed numerous projects successfully and currently managing a couple of real-world AI based funded projects. Her research interests include Computational Physics, Theoretical Physics, Medical Physics, Atomic, Molecular and Optical Physics, Optics, and Condensed Matter Physics.